A Geochemical Review of Amphibolite, Granulite, and Eclogite Facies Lithologies: Perspectives on the Deep Continental Crust

Laura G. Sammon[1], **William F. McDonough**[1,2]

[1]Department of Geology, University of Maryland, College Park, MD 20742, USA
[2]Department of Earth Sciences and Research Center for Neutrino Science, Tohoku University, Sendai 980-8578, Japan

Key Points:

- We synthesize, analyze, and reported statistics on $\sim 10,000$ whole rock, literature compositions for deep crustal lithologies.
- We determine periodic table trends and implications for composition of the deep continental crust.
- We generate middle, lower, deep, and bulk crust compositional models.

Keywords: Geochemical modeling, granulite, amphibolite, eclogite, deep crust, lower crust, middle crust

Index Terms: 1009 Geochemical modeling (3610, 8410), 1020 Composition of the continental crust, 1065 Major and trace element geochemistry, 3640 Igneous petrology, 3660 Metamorphic petrology

Author ORCID numbers are

Laura G. Sammon : 0000-0002-4538-0700
Willaim F. McDonough : 0000-0001-9154-3673

Corresponding author: Laura G. Sammon, lsammon@umd.edu

Abstract

Debate abounds regarding the composition of the deep (middle + lower) continental crust. Studies of medium and high grade metamorphic lithologies, which serve as analogues, guide us but encompass mafic (< 52 wt.%) to felsic (> 68 wt.%) compositions. This study presents a global compilation of geochemical data on amphibolite (n = 6500), granulite (n = 4000), and eclogite (n = 200) facies lithologies (xenoliths and terrains) and quantifies systematic trends, uncertainties, and sources of bias in the deep crust sampling. The continental crust's Daly Gap is well documented in amphibolite and most granulite facies lithologies, with eclogite facies lithologies and granulite facies xenoliths having mostly mafic compositions. Igneous differentiation processes likely dominate the formation of the compositional layering seen in the crust. Al_2O_3, Lu, and Yb vary little from top to bottom of the crust. In contrast, SiO_2, light rare earth elements, Th, and U show a wider range of abundances throughout. Because of oversampling of mafic lithologies, our predictions are a lower bound on middle crustal composition. Additionally, the distinction between granulite facies terrains (intermediate SiO_2, high heat production, high incompatibles) or granulite facies xenoliths (low SiO_2, low heat production, low incompatibles) as being the best analogs of the deep crust remains disputable. We have incorporated both rock types, along with amphibolite facies lithologies, to define a deep crustal composition that approaches 57.6 wt.% SiO_2. This number, however, represents a compositional middle ground, as seismological studies indicate a general increase in density and Vp and Vs velocity with increasing depth. Future studies should analyze more closely the depth dependent trends in deep crustal composition so that we may develop composition models that are not limited to a three-layer crust.

Plain Language Summary

The composition and origins of the bottom $\frac{2}{3}$ of the continental crust has been a topic of geologic debate for many years. Because of the inaccessible depths of these middle and lower sections of the continents, we cannot sample them directly. We must rely on rocks brought to the surface through mountain building and magma entrainment processes. Deep crustal rocks delivered via these processes come from a wide variety of depths and encompass many different chemical compositions. This study seeks to understand and better characterize the average composition of the deep crust (typically from 15 to 40 km beneath the surface) and identify the processes that produced the crust's present-day, chemically layered structure.

1 Introduction

The composition of the deep continental crust has been the subject of many studies for the past half century because of its importance in crustal evolution and the lack of consensus on its composition. The combined middle and lower continental crust (referred to here as the "deep crust") are the integrated chemical products of billions of years of crust formation and deformation, yet their inaccessibility (deeper than 10 km) has led to a poorly constrained compositional model for the lower two-thirds of the continent. The deep continental crust can be sampled through tectonically emplaced exposures of high-grade metamorphic rock (referred to here as "terrains") or deep crustal xenoliths that are rapidly carried to the surface through volcanic eruptions. The composition of these deep crustal analogues ranges widely, encompassing lithologies from metamorphosed basalt to granite. Varied tectonic regimes and widespread crustal heterogeneity have led to numerous geochemical and geophysical models that help to explain local phenomena, but struggle to produce a coherent global picture. Attempts to resolve the debate are limited by nonunique solutions and poorly quantified uncertainties. Defining the bulk compositional properties of the deep continental crust and describing its depth depen-

dent changes endures as a long-standing challenge. Thus, the deep crustal composition puzzle remains, troublingly, unsolved.

Rudnick (1995) posited the paradox of the continental crust: the continental crust has an andesitic composition, however melts from the mantle are basaltic. In doing so, she identified that the formation of continental crust, as compared to making oceanic crust, must be an open system process involving, to different extents, weathering, intracrustal melting (leaving behind a dense residue), and delamination as some of the operating processes. Consequently, the geochemical uncertainty associated with deep crust composition has led to competing models for crust formation (Bürgmann & Dresen, 2008; Rudnick & Gao, 2014; Hacker et al., 2015).

In developing their model, Hacker et al. (2015) outlines two processes that they envisage as shaping crustal evolution: delamination and relamination. Delamination occurs when gravitationally unstable material in the deep crust, such as eclogite and other garnet-rich lithologies, separates and flows into the less dense underlying mantle. This process leads to a dense, mafic deep crust as eclogitization occurs but before the lower crust delaminates. In contrast, the process of relamination thrusts subducting sediment under the continental crust, resulting in a more felsic, less dense lower crust. While individual examples can be found to support each of these processes, the difficulty remains in determining the dominant pattern of crust evolution.

The continental crust is conventionally split into upper, $\pm$ middle, and lower layers, though distinct seismic or petrological/geochemical boundaries are not always evident (Holbrook et al., 1992). Petrological and geochemical studies of the deep continental crust have therefore sought to define its composition through analysis of various high grade metamorphic lithologies. It is difficult to gauge, however, if isolated metamorphic samples are representative of the entire deep crust. Temperature and pressure, and therefore metamorphic grade, increase with increasing depth in the crust, though the geothermal gradient varies by up to a factor of $\sim$ 3 depending on continental crust type and tectonic regime (Christensen & Mooney, 1995). If a pressure of 1 GPa is reached at 35 km (assuming an average crustal density of 2,900 kg/m^3 (Wipperfurth et al., 2020)), the deep crust could plausibly be composed of greenschist, amphibolite, granulite, and/or eclogite facies lithologies. However, amphibolite and granulite facies material dominate what are interpreted as deep crustal cross-sections (such as metamorphosed terrains exhumed in the Ivrea-Verbano Zone, Italy), with minimal evidence for greenschist facies lithologies (Rudnick & Gao, 2014). Eclogite facies lithologies likely contribute to orogenic regions with thickened deep crust (pressures up to 1.5-2 GPa following the same density scheme as above)(Lombardo & Rolfo, 2000; Leech, 2001). For these reasons, this study focuses on amphibolite, granulite, and eclogite facies lithologies as potential major components of the deep crust. We report on an expanded database developed by Rudnick and Presper (1990) and added to by Hacker et al. (2015), including data sourced from Earthchem.org; we examine the chemical trends among various medium to high grade metamorphic lithologies to understand and better characterize what is the average composition of the deep continental crust and follow this with implications for crustal differentiation and evolution processes.

2 The Art and Science of Deep Crustal Modeling

In many ways, predicting the composition of the deep continental crust is as much an art as it is a science, because deep crustal models depend not only on the input data, but also the approach each modeler takes to interpreting said data. The definition of the deep crust depends on the question each researcher is trying to address, and is therefore neither a static nor universal term. This can sometimes lead to confusion and produce seemingly contradictory models of the crust when in fact, each model is simply looking at the crust through a different lens.

How many layers should we split the crust into? What is the scale of lateral variations in the crust? The answers differ based on the model. This fundamental question is the crux of the disagreement between popular composition models (e.g., Rudnick & Gao, 2014; Hacker et al., 2015). While some split the crust into two layers (e.g., Hacker et al., 2015), upper and lower, shallow and deep, others split it into three (upper, middle, and lower) or more sections (Christensen & Mooney, 1995; Mooney et al., 1998). Thus, debates about compositional models need to be clear about their specific crustal mass fractions. Much geophysical effort has gone into determining the layering and seismic structure of the continental crust. Such topics are beyond the scope of this study, but we want to bring the concept of model resolution to the readers' attention so that they can appreciate the complexity of the task of modeling deep crust composition and be mindful that we are taking but one approach.

2.1 A Forward Model, an Inverse Model

Classically, two approaches have been taken to assess deep crustal composition: sample driven modeling and process driven modeling. Sample-driven models base their conclusions on the premise that deep crustal analogue samples, such as mafic high grade metamorphic xenoliths, are by and large representative of the composition of the deep crust. Empirical analyses are the main source of data for this type of model. This geochemical inverse model takes measured element concentrations from surface rocks and derives the conditions under which they formed. A second approach considers physical processes and constraints that build the deep crust and the effects of crust formation and evolution. A variety of mafic and felsic compositions can satisfy the geophysical observables, such as Vp or viscosity (e.g., Hacker et al., 2015; Shinevar et al., 2018). These forward process models consider all possible geochemical solutions, avoiding the potential bias of xenoliths, which may be sampling a restricted portion of the deep crust, or whose chemistry has been influenced by their limited eruption environments. Both approaches have their strengths, and in the end, both can be considered correct.

This study more closely resembles the first approach, using samples to infer deep crustal composition. We are mindful of the potential biases this leads to (refer to Section 3.2). For the sake of comparison to other models, we operate under the assumption of a three-layer crust, though we advocate for embracing the potential for vertical and lateral compositional variation by analyzing the full spectrum of available data. Future studies should move beyond bisecting or trisecting the crust, taking advantage of the quality and resolution of both geochemical and geophysical data currently being produced.

3 Datasets

3.1 Amphibolite, Granulite, and Eclogite

For the rest of this study, "amphibolite", "granulite", and "eclogite" will be characterizations of chemical metamorphic grade, with few constraints on absolute composition. Both amphibolite and granulite facies lithologies range from mafic ($<$ 52 wt.% SiO_2) to felsic (>68 wt.% SiO_2) in composition, and can have Mg#'s (molar $\frac{Mg}{Mg+Fe}$) that resemble the mantle (Mg# $\sim$ 89), the upper continental crust (Mg# $\sim$ 30), or any number in between. Eclogite facies lithologies are less heterogeneous than amphibolite or granulite facies. Eclogite facies mineral assemblages are dominated by (clino)pyroxene and garnet, leaving less room for variations in silica content. Please note that "eclogite" as a metamorphic grade is less restrictive in composition than the largely garnet-omphacite, bi-mineralic rock, eclogite.

The medium pressure (e.g., 0.2-0.8 GPa) and temperature (e.g., 200-600°C) metamorphism of amphibolite facies lithologies presumably reflects the conditions of the middle continental crust. Granulite facies lithologies are widely held to comprise the lower

continental crust, with its base being defined seismically by the Moho. Amphibolite facies lithologies are generally sampled through surface-exposed terrains and are more rarely sampled through xenoliths. Granulite facies lithologies can be sampled via terrains or xenoliths. Granulite facies xenoliths have predominantly mafic to intermediate-mafic (45 - 55 wt.% SiO_2) silica content, while granulite facies terrains span the range of mafic to felsic. Granulite facies rocks are distinguished from amphibolite facies rocks by the dehydration of hydrous mineral phases (Rudnick & Fountain, 1995). The water-rich minerals that can occur in amphibolite, such as amphiboles and micas, break down into pyroxenes in the granulite stability field due to higher temperatures. Granulite facies metamorphism initiates around 600°C, meaning that any granulite facies rocks present in areas where the crust is thin and/or the lower crust is at temperatures < 600°C are likely in thermal disequilibrium. Granulite facies lithologies, however, are only expected to undergo retrograde metamorphism under limited circumstances due to the kinetic barrier of rehydration (Semprich & Simon, 2014). Thus, many studies still use metastable granulite as a lower crustal analogue.

The eclogite facies is traditionally bounded by the pressures and temperatures required to transform basaltic mineral assemblages into clinopyroxene and garnet $\pm$ rutile $\pm$ accessory minerals. Though it can be difficult to achieve the pressures required to form eclogite in average continental crustal settings (crustal thicknesses < 40 km), eclogite facies materials may be a significant component of modern and paleo-orogenic belts (Leech, 2001; Lombardo & Rolfo, 2000).

3.2 Potential Biases

The first step in analyzing a dataset is to admit that it is potentially biased. Throughout this paper, we scrutinize the statistical uncertainty of deep crust compositions. Systematic uncertainties, however, are not so easily quantified. This section offers what limited insight we have on the potential for systematic bias in our deep crust sample set. The analyses and conclusions in the rest of this paper are generally founded upon the assumption that the following systematic biases have a limited effect on our dataset, and if any datasets do fall prey to bias, they can be amended without significantly changing the overall picture of deep crust composition.

Our compendium of deep crustal samples, available in the supplemental information of this paper, consists of published data from various sources, most of which are available on Earthchem.org (`www.earthchem.org`). We used a subset of the data available, limiting our calculations and analyses to samples whose major oxide content is reported and totals to 100 $\pm$ 10%. Because of the numerous opportunities for bias in our dataset, we only limited samples by metamorphic grade and major oxide totals. Removing the oxide totals filter does not substantially change the distributions of most elements, but tends to increase the data scatter. The filtered and unfiltered data sheets are available as supplemental information.

3.2.1 Location Bias

The global distribution of medium and high grade metamorphic samples shows little correlation between composition and location (Figures S1 and S2). In fact, samples of mafic and felsic compositions are often found within the same region. We are, of course, limited to areas where terrains and/or xenoliths have been exposed at Earth's surface, but our data include samples from all seven continents. Amphibolite facies lithologies have been extensively studied in crust of various ages. Granulite facies lithologies are also widely sampled, though the xenoliths are relegated to areas that have experienced uncommon eruptions of mafic, xenolith-bearing magmas. In addition, Archean granulite facies terrains are generally restricted to cratonic regions. Eclogite facies xenoliths and terrains are our most limited datasets, but >200 samples are still available for study. Many

eclogite facies samples are from the western United States, potentially biasing the dataset towards the lawsonite eclogites of the Franciscan Complex and eclogites formed from oceanic crust subduction (Tsujimori et al., 2006). South America and Antarctica are not represented in the eclogite facies dataset.

3.2.2 Buoyancy and Transport Mechanism Bias

The deep crust may not be fully represented by the *analogue* samples that have reached Earth's surface. Medium and high grade metamorphic lithologies that have survived surface transport do not necessarily reflect the full distribution, abundance, or composition of the deep crust. Felsic terrains could be over-represented at the surface due to their lower densities. Buoyancy is a significant dynamical force that may play a critical role in determining what types of metamorphic terrains outcrop at the surface (Kelemen & Behn, 2016; Gerya et al., 2002).

On the other hand, eruption type and location may likewise bias xenolith compositions (Jaupart & Mareschal, 2003), including contaminating them with the basaltic lavas. (Rogers & Hawkesworth, 1982; Rudnick & Taylor, 1987a; Rudnick & Presper, 1990). Studies have also found that felsic xenoliths often cannot withstand the frequently hot, violent eruptions that transport samples to the surface and tend to be re-assimilated (Halliday et al., 1993; Rudnick & Fountain, 1995). Granulite facies xenoliths in particular could be biased by location and/or eruption method: they tend to be co-located with cratonic crust because they are often carried by kimberlite eruptions and fast-erupting alkali basaltic volcanism (Russell et al., 2012; Rudnick & Presper, 1990).

3.2.3 Preservation and Exposure Bias

We recognize also the potential of sample preservation bias. Recent studies outline different weathering rates for different metamorphic rock compositions (e.g., Price & Velbel, 2003; Ohta & Arai, 2007). Age and weathering rate, along with protolith composition, may affect the current metamorphic sample population.

Metastable conditions in the deep crust are another concern. Granulitic lithologies would not be in thermal equilibrium under most projected geotherms (e.g., Kusznir & Park, 1987). In fact, the middle continental crust should be stable in the greenschist facies and the lower crust in amphibolite facies, but this lower grade combination is not often observed in exposed cross-sections (Rudnick & Gao, 2014). On average crustal cross-sections are dominantly from $\leqslant$30 km depth (Table 4 in Rudnick & Gao, 2014). These are comparble with high temperature/pressure metamorphism, which has a mean pressure of 0.8 GPa (i.e., 25-30 km depth) and are associated with double thickened crust (Brown & Johnson, 2019). The abundance of amphibolite and granulite facies material in (what we deem to be) deep crustal cross-sections suggests that the deep crust reached peak metamorphic conditions some time in the past and has since cooled off. We choose to classify this observation as a "preservation bias" because we are preferentially preserving metastable mineral assemblages.

3.2.4 Sample Collection and Naming Bias

Lastly we face the bias that we as scientists impose ourselves: collection and classification bias. Unique localities can be over-sampled for their novelty, and thus, overly abundant in the dataset. Common andesitic rocks, with their lack of attractive phenocrysts and dull grayish-pink hue, may unfortunately be glossed over in favor of more attractive samples (apologies to Dr. J. Blundy and colleagues). Oversampling the same locations seems to plague the amphibolite facies dataset most, with many nearly identical samples in Japan, Alaska, the western United States, and the Appalachian region of the eastern United States. We look more closely at the consequences of this redundant sam-

pling in Section 8. However, for the main analysis of amphibolite facies lithologies in this paper, we keep all amphibolite facies samples in the datasets so that we can see the full span of available data.

Even if we have done our due diligence, we also unintentionally bias samples by our classification schemes. Metamorphic lithologies can be categorized by texture (e.g., schist, gneiss) or pressure-temperature (P-T) grade (e.g., amphibolite, granulite), and incomplete changes in lithology can lead to subjective naming. We can estimate the P-T grade of the deep crust through mineralogy, but would need geophysical measurements to assess its schistocity or anisotropy (Godfrey et al., 2000). The database contains sample data named for their chemical metamorphic grade in some cases and named for their texture in other cases. Samples defined by their metamorphic texture (e.g. gneisses) have been assigned manually to the amphibolite or granulite facies based on the metadata available and publications associated with these samples. Unfortunately, >6000 gneisses, schists, and meta-igneous samples could not be included in this study because there was not enough information to discern their chemical metamorphic grade. Metamorphic texture on its own, without mention of stable mineral assemblages, cannot be correlated to precise P-T conditions.

To mitigate the oversampling of individual geologic formations, we averaged all samples collected within 0.2deg x 0.2deg latitude x longitude of each other. This averaging did not change the median composition of granulite facies xenoliths. The median composition of eclogite facies xenoliths and terrains, and granulite facies terrains of all ages changed by $< 4\%$. For amphibolite facies lithologies, however, the median composition, especially SiO_2, increased drastically by $>10\%$.

While an unknown amount of bias plagues our dataset, over 10,000 samples contribute to our understanding of deep crustal composition. Systematic differences among the different metamorphic lithologies are discussed in the appropriate sections. These differences, where quantifiable, serve as markers for different possible deep crustal compositions. This study focuses on a contextualized overview of compositional aspects; it does not delve deeply into metamorphic processes. Should any systematic errors fundamentally shift our understanding of the deep crust, that in and of itself would be worthy of future assays.

4 Major Element Compositions

4.1 SiO_2, MgO, FeO, and the Daly Gap

The abundance of major oxides in deep crustal analogue samples is difficult to summarize with a single value and uncertainty. Elemental distributions are not always well defined by the convenient-to-describe Gaussian, normal, log normal, or gamma distribution functions. Table 1 reports summary statistics for amphibolite, granulite, and eclogite facies lithologies major oxide content, but are by no means the most comprehensive descriptions of these complex distributions. Unless indicated otherwise, we will reference the median $\pm \frac{1}{2}$ the interquartile ranges because of their resistance to skewness and outliers.

A discussion of the significance of median versus mean should also include the practice of evaluating element ratios. Should one consider the representative element ratio to be represented by a ratio of the means or a mean of the ratios? (Likewise, be represented by a ratio of the medians or a median of the ratios?) There is no simple answer to this question; it has been debated extensively without reconciliation. The fundamental question asks – how representative is one's data set of the geological domain being evaluated? For the deep crust, there are many unknowns including unknown unknowns. Hence our preference is to use median values and a median of the ratio, as these resist the influence of skewness and outliers.

Because the distributions of major oxides tend to be skewed and/or multi-modal, our oxide totals are between 90 and 95% when summing the means or medians. We delve further into assessing the modality of our distributions in Supplement S.1. Supplemental tables ST1 - ST6 list distribution parameters and summary statistics for all elements. We acknowledge our hubris in attempting to parameterize non-parametric distributions, but we are condemned to using bite-sized descriptions of data in the somewhat Sisyphean task of quantifying the chemical composition of a crust we cannot easily access.

The most noticeable data trend is the bimodal distribution of primitive and evolved samples, illustrated by Figure 1. The phenomenon published by Rudnick and Presper (1990) persists in this dataset of over 4,000 granulite facies samples and is also present in over 6,000 amphibolite facies samples. Granulite facies xenoliths are dominantly mafic, having <55 wt.% SiO_2 and ranging from mantle-like Mg#'s $\sim$ 89 to Mg#'s of 45-50. Granulite facies terrains encompass both mafic and felsic compositions. The felsic samples follow a Fe-enrichment/Mg-depletion trend, leading to a double-peaked structure, resembling a chair, when plotted in Mg# vs. SiO_2 space. There is also an age-dependent trend in composition within the granulite facies terrains dataset: older, Archean samples are more evolved than Post-Archean samples. Amphibolite facies lithologies show the same chair-like structure, but with a greater concentration of mafic samples. No distinction is made between amphibolite facies terrains and xenoliths in the dataset because of the scarcity of amphibolite facies xenolith data.

The corollary to this bimodality is the "missing" intermediate samples between 53 and 68 wt.% SiO_2. The Daly Gap (Daly, 1914) describes the lack of intermediate compositions observed in *all* 700,000 metamorphic and igneous samples in the *Earthchem.org* database. Thermodynamic instability of intermediate compositions (Daly, 1914; Dufek & Bachmann, 2010) and liquid immiscibility (Reubi & Blundy, 2009; Charlier et al., 2011), among other hypotheses (Jackson et al., 2018; Yamasaki, 2018), have been proposed to explain the gap. While it is possible that these rocks are not representative of the crust, we conclude that this is dubious given its coherence across multiple lithologies.

The systematically mafic composition of granulite facies xenoliths was noted by Rudnick and Presper (1990) along with many other studies thereafter. Among the proposed explanations for the relative abundance mafic xenoliths are that felsic xenoliths are less likely to survive the eruption process (Halliday et al., 1993; Rudnick & Fountain, 1995) and that xenoliths might sample deeper regions of the crust than terrains (Bohlen & Mezger, 1989; Rudnick & Fountain, 1995). Terrains, on the other hand might be biased towards sampling shallower or more felsic regions because mafic terrains are less buoyant and less likely to reach the surface (Gerya et al., 2008). Granulite facies terrains also show aged-based compositional biases, with Archean samples (61.5 $\pm$ 8.5 wt.% SiO_2) being, in general, more evolved than Post-Archean samples (61.5 $\pm$ 8.5 wt.% SiO_2) despite having similar median values. Studies have suggested that the ages recorded in these high grade metamorphic samples have been affected by open system behavior (Ashwal et al., 1999) or, as more traditionally argued, hotter temperatures in the Archean allowed for greater amounts of delamination of mafic material, leaving the Archean crust enriched in felsic components (Martin, 1986).

There is no discernible compositional difference between granulite facies terrains and xenoliths of comparable SiO_2. Most other compositional trends, such as elevated median CaO in granulite facies xenoliths or rare earth element enrichment in terrains (discussed later), correlate to the sample's silica content. The composition of granulite facies lithologies seems to have little dependence on location (other than the fact that xenoliths are generally most accessible in regions that have experienced volcanism); if surface transport mechanisms are affecting the composition of these granulite samples, then they are not doing so beyond preferentially selecting for certain SiO_2.

The strong preference for mafic compositions in amphibolite facies lithologies is likely biased by mineralogy and geologic naming conventions. Amphibolite facies lithologies unsurprisingly contain amphibole minerals, which generally form in mafic rock compositions. Felsic rocks of similar metamorphic grade seem to be categorized as schists, gneisses, or even metapelites. It is likely that many amphibolite facies samples were excluded from our study because they were given a textural metamorphic grade designation. Thousands of intermediate and felsic gneisses could not be assigned to amphibolite or granulite facies because of insufficient metadata.

The eclogite facies xenoliths and terrains are limited to 46.2±1.2 and 47.2±2.2 wt.% SiO_2, respectively. This is likely due to the stricter definition of "eclogite", which can refer to a bi-mineralic rock or require basaltic mineral assemblages to reach high pressure. Eclogite facies lithologies have Mg# of 30 to 90, with no correlation to location or method of surface transport.

4.2 The Constancy of Al and Ga

Notably, Al_2O_3 content remains relatively constant (i.e., ∼12% variation) throughout all samples. Though eclogite facies lithologies have slightly elevated Al_2O_3 content compared to the other samples (Table 1), estimates for Al_2O_3 only range from 14-17 wt.%. The Al_2O_3 values of granulite facies lithologies are roughly 5-15% lower than the commonly accepted lower crustal Al_2O_3 values of Rudnick and Gao (2014) though still within the study's given error. Our estimated Al_2O_3 content in granulite facies lithologies are more in line with Wedepohl (1995) and Gao et al. (1998) lower crustal values.

Elements of the same group in the periodic table tend to behave similarly. For example, the abundance of Ga tracks with Al and Ge tracks with Si (De Argollo & Schilling, 1978). Comparable to Al, Ga concentrations are nearly constant in amphibolite and granulite facies lithologies: median abundance ranges from 17.3 to 19.5 ppm. Eclogite facies samples again behave differently. Due to the significantly smaller sample sizes of the eclogite lithologies. There is little or no data reported for Ge and so we predict its concentration in the deep crust to be relatively invariable at about 1.3-1.4 ppm, based on chemical trends for igneous rocks (De Argollo & Schilling, 1978).

4.2.1 Understanding Protolith Populations

A comparison of the molar abundances of Al to alkali metals and alkaline earths provides a potential provenance indicator for the origin of deep crustal rocks. Sedimentary rocks typically have Al_2O_3 contents of ∼20 wt.% (Taylor & McLennan, 1985), whereas most igneous rocks vary from 12 to 19 wt.% Al_2O_3 (De La Roche et al., 1980). Anorthosites and other plagioclase-rich cumulate rocks, however, can have much higher Al_2O_3 contents.

Al content and Aluminum Saturation Index have in the past been used to help infer the protolith of deep crustal samples. When a rock's Aluminum Saturation Index (ASI; molar $Al_2O_3/(CaO + Na_2O + K_2O)) > 1$, it is classified as peraluminous (Zen, 1988), but with no characterization of its source of origin, so caution is needed. Though sedimentary rocks tend to have higher Al contents (ASI = 1.12, Earthchem.org data, sedimentary rock data, excluding carbonates), Zen (1988) reported granites having ASI values between 1 and 1.4 and noted that these rocks can be derived from a variety of source lithologies, with the proviso that for large bodies of strongly peraluminous granitic rocks peraluminous sources seem necessary. Chappell et al. (2012) observed that many I(igneous)-type granites are peraluminous and owe their origins to partial melting of more mafic source rocks. They also noted that gradations from peraluminous felsic granites to metaluminous igneous compositions are seen for rock suites that have a shared, closed isotopic system.

Unknowns remain significant regarding the amounts of and the depths to which sedimentary lithologies are transported into the deep crust. Our samples have median ASI values ranging from 0.65 to 1.06, yet the distribution of aluminous indices is wide and sometimes asymmetrical (Fig. 2). Amphibolite facies lithologies and granulite facies xenoliths have ASI values comparable to igneous lithologies (Earthchem.org data, median ASI = 0.76). Eclogite facies lithologies have a median ASI values lower than the median igneous ASI. Crustal recycling into the mantle is a well established feature of plate tectonics. Surface sediments and foreland basin molasse deposits cover crystalline materials in convergent margin, but these readily deformable sedimentary units are typically scraped off and not deeply recycled.

No metric seems perfect for identifying a deep crustal rock's protolith type. Hacker et al. (2015) identified 44% Archean and Post-Archean granulite-facies rocks as peraluminous and noted that they may be metasedimentary; going further, they suggested that amphibolite-facies terrains have similar statistics and that 16% granulite-facies xenoliths that are peraluminous may be metasedimentary. We do not find compelling evidence that the ASI value provides unambiguous indication of what is a metasediment. In fact, as cautioned by Chappell et al. (2012), many peraluminous rocks are igneous, including those derived from the remelting of igneous rocks. Given that the term peraluminous does not effectively identify what might be a metasediment, we turned to a machine learning algorithm to predict a metamorphic protolith from major element chemistry (Hasterok, Gard, Bishop, & Kelsey, 2019). This method, however, also produced unclear results. The algorithm showed low confidence in whether the protoliths were igneous or sedimentary, with ratings close to 0 instead of -1 (confidently igneous) or 1 (confidently sedimentary). A broader view of factors must be considered to determine the formation and evolution processes of the deep crust.

5 Minor and Trace Element Composition

Here we discuss key geochemical trends seen in incompatible elements; other observations are not covered here for the sake of brevity. The rest of the data is addressed in more detail in Supplement S.2, which reviews our findings for fluid mobile elements, high field strength elements (HFSE), transition metals, and other important groups of elements. Regardless of surface transport mechanism (eruption as xenoliths or tectonic emplacement as terrains), there are no differences in trace element content between granulites of similar SiO_2 content. Therefore, granulite facies xenoliths and terrains can be treated as one lithology when discussing silica-correlated compositional trends. Eclogite facies xenoliths and terrains have fewer data points, so it remains unclear whether or not they should be given the same treatment.

5.1 Rare Earth Elements

Figures 3 and 4 illustrate that the rare earth element patterns of all of the samples are congruent, having greater variation in the light rare earths (LREE) and than in the heavy rare earth elements (HREE). The amphibolite and granulite data show LREE enrichments and their variability is comparable to that shown by Rudnick and Gao (2014), with granulite facies terrains having the highest median concentrations of La through Nd. Igneous processes - rather than metamorphic changes or chemical weathering - control the relative enrichment in LREEs seen in granulite facies terrains compared to granulite facies xenoliths or amphibolite lithologies. The greatest abundance of La and Ce is not seen in the most hydrated samples (amphibolites) but in the most evolved samples (granulite facies terrains). Eclogite facies lithologies are relatively depleted in LREE compared to amphibolites, yet they are more enriched than granulite facies xenoliths. The standard deviation of the REE distributions narrows from La to Lu. Eclogite facies samples surprisingly show no relative enrichments in HREEs, which would be typ-

ical of rocks with more abundant garnet. The HREEs concentrations, especially Tm, Yb, and Lu are identical for all of the metamorphic facies in question.

Amphibolite facies lithologies and granulite facies xenoliths span similar ranges of La/Yb, 8.16 ± 6.5 and 7.52 ± 3.2, respectively. Archean granulite facies terrains have a much higher median value (La/Yb = 16.0 ± 10.2) than Post-Archean terrains (La/Yb = 10.1 ± 4.50) despite having similar SiO_2 content, yet La/Yb and is correlated to SiO_2 and forms the same chair-like structure when in natural log La/Yb space as SiO_2 vs. Mg#. The bimodal structure suggests that the Daly Gap affects La/Yb, and that the ratio reflects the original igneous processes that formed the rock rather than metamorphism or weathering.

Flatter rare earth patterns (lower La/Yb ratios), common among the eclogite facies xenoliths and terrains, do not seem to be relegated to specific regions. It is possible that eclogite facies terrains are biased by alteration and subduction processes despite how closely they resemble xenoliths because of our limited dataset (e.g., Tsujimori et al., 2006). As mentioned earlier, many of our eclogite facies terrains samples originate from areas that have evidence of significant subduction, such as the western United States. Eclogite facies terrains from the Caledonides in Norway (e.g., Rockow et al., 1997; Svensen et al., 2001) also show REE variation even within the same formation. Sampling exposures of eclogite facies terrains in regions that have not been subjected to significant amounts of subduction would provide more clarity - if such terrains exist. The apparent enrichment in Gd, Dy, Ho, Er, and Tm in eclogite facies terrains is due to our limited dataset, with those elements having only 1 to 5 datapoints each.

On average the crust shows a systematic vertical concentration gradient in REE abundances (i.e., UC → MC → LC, showing La 36 → 18 → 12; Yb 3.1 → 2.2 → 1.7 ppm), with a mildly fractionated downward decrease in the LREE (factor of 3) and HREE (factor of 2). Likewise, Eu/Eu* changes from a 30% negative anomaly in the upper crust to essentially no anomaly in the lower crust. These compositional gradient are most likely products of intracrustal differentiation, with granite magmas moving upward and residuals being stored in the lower crust or lost to the mantle via gravitational processes.

5.2 Heat Producing Elements

Heat producing elements (HPEs: K, Th and U) are of particular interest because they are crucial to understanding Earth's radioactive heat budget (these three elements produce 99.5% on the radiogenic heat) through time as well as the temperature and strength of the crust. Rudnick and Gao (2014) estimate the continents host 35 to 40% of the Earth's budget of HPE. Constraining Earth's HPE abundances (especially the abundance of the refractory lithophiles, e.g., U and Th) also constrains ∼26 other elements (McDonough & Sun, 1995) that are in conserved, chondritic ratios relative to U and Th.

5.2.1 Th, U, and K

As has been recognized for the last half century (Rudnick & Gao, 2014), HPE abundances decrease from the upper crust to the Moho. The behavior HPE can often be understood through comparisons of elemental ratios. About 80% of the Earth's total heat production comes from Th and U and thus the Th/U ratio is key. Wipperfurth et al. (2018) recently reviewed Th/U values for ∼150,000 crustal rocks and sediments and found that the median values for igneous and metamorphic rocks were close to the bulk Earth's value of 3.8. We find that amphibolites have a median Th/U of 3.7, whereas granulite terrains appear to have lost U (see below) relative Th (median Th/U for Archean and Post-Archean granulite terrains are 7.3 and 6.6, respectively). In contrast, however, the median Th/U of granulite xenoliths (3.4) appears to be normal (i.e., no U loss). There is little correlation between K content and K/U, with median K/U values for all metamorphic litholo-

gies ranging upwards of one to three times that of upper continental crust. We observe K/U values from 10,000 to 100,000 with uncertainties on the order of 60%. Whether K behaves as a trace element or thermodynamic component (i.e., mineral) controls the K abundance in our samples. That is, K values are high if K-feldspar is present in the system, whereas values are low if K-feldspar is not present. The K/Th value is relatively constant in deep crustal lithologies and similar to that of the upper crust (Rudnick & Gao, 2014), implying K/U fractionation is due to U loss, not K loss, and confirming the earlier finding of Rudnick and Presper (1990).

A question that remains is, when did this uranium loss occur in the granulite terrains? To address this issue we combined the two separate measures of Th/U. The isotopic ratio of ^{232}Th/^{238}U value is referred to as κ ($\kappa \sim$ Th/U $\times$ 1.033), while the time-integrated Pb isotopic ratio ($^{208}Pb^*/^{206}Pb^*$, the decay products of ^{232}Th/^{238}U) is κ_{Pb}, which serves as a proxy for Th/U. [κ_{Pb} values are calculated from the measured lead isotopic composition of the sample minus its primordial lead contribution; see details in Wipperfurth et al. (2018).] The κ_{Pb} provides a measure of the time-integrated Th/U value and is resistant to recent resetting. The average (and median) κ_{Pb} for the amphibolites, granulite xenoliths, and Archean and Post-Archean granulite terrains is 4.1$\pm$0.1 (4.0$\pm$0.1; n=165, 357, 33, and 4, respectively), while eclogite xenoliths are 5.5 (5.8; n=21) and no data for eclogite terrains; see appendix Table 3 for further details. The $\sim$70% difference between Th/U and κ_{Pb} values for granulite facies terrains is consistent with a recent uranium loss. On average it appears that surface exposure results in the loss of U from the granulite and less so due to dehydration metamorphism.

In general, U and Th show positive correlations with SiO_2. Mean and median U and Th values increase with increasing SiO_2 abundance for amphibolite and granulite facies rocks. While the relationship between SiO_2 and U or Th is log-normal within uncertainties, the concentration of U and Th could potentially also be derived from SiO_2 through a probability analysis (e.g., Hasterok, Gard, Cox, & Hand, 2019; Gard et al., 2019).

Deep crustal heat production is but a fraction of upper crustal heat production. The median heat production in the deep crustal lithologies ranges from 0.04 to 0.41 nW/kg (roughly 0.1 to 1.2 μW/m^3, assuming a density of 2900 kg/m^3). Post Archean granulite facies terrains have the highest heat production to 0.4 $\pm$ 0.5 nW/kg ($\sim$1.2 μW/m^3). How we calculate our heat production is significant: the *mean of the averages* does not equal the *average of the means*. Using the median K_2O, Th, and U abundances, we calculate heat production for Post-Archean and Archean granulite facies terrains to be 0.14 and 0.15 nW/kg (0.41 and 0.42μW/m^3), respectively. The answer lies in the shape of the distributions, which are neither normal nor log-normal. In this case, our simplified statistics are sub par descriptors of the datasets. Yet, we see that median deep crustal heat production should be minimal unless there is significant incorporation of granulite facies terrain material.

6 Distributions that Trend, Periodically

The periodic table is a wonderful tool to use when analyzing elemental trends because of its structure and organization. It shows that elements of similar valence states and radii behave predictably and highlights anomalies caused by specific minerals or sampling methods. We expect to see more skewed distributions for elements that change abundance with depth, since our dataset possibly includes samples from a range of depths (Bohlen & Mezger, 1989). The difference between mean and median is one metric for quickly assessing the shape of non-normal distributions. McDonough (1990) found that major and compatible trace elements have similar average and median values, whereas median values are systematically lower than average values for the incompatible trace elements (e.g., LREE, K, Rb), with differences between average and median values increasing with in-

creasing incompatibility. Figures 5 and 6 are color coded to show the % difference between mean and median for amphibolite and granulite facies lithologies. The same methodology can be applied to eclogite facies lithologies, but the distributions are more discontinuous, and trends are less clear due to having an order of magnitude fewer samples. Even in the amphibolite and granulite datasets, elements with relatively few data points (such as the highly siderophile elements) appear highly skewed.

Al and Ga are unimodal, with little variation in their abundances compared to other elements, and Na is relatively constant, with some possible bimodality. The mean and median values for Si are similar because of its bimodal distribution, but we do not find conclusive evidence for bimodality in other oxides. Fe, Mg, and Ca show some degree of multi-modality. Most of other elements in the table are unimodal. The rare earth elements exhibit consistent patterns between amphibolite and granulite facies lithologies, though amphibolites have greater differences between mean and medium in the light rare earth elements. The homogeneous purple colors among the rare earths underscores their predictable behavior, with the greatest skewness occurring in the light rare earths (most pink on the mean - median scale) and tapering off to a steady ∼10% difference between mean and median towards the heavy rare earths.

Both Th and U have highly skewed distributions that verge on log-normal for both amphibolite and granulite facies lithologies. The distributions of U and Th in granulite facies terrains are indistinguishable from both a gamma and a log-normal distribution (using a Wilcoxon rank sum test of median values). The distributions of U and Th in granulite facies xenoliths and amphibolite facies lithologies, however are more accurately described by log-normal distributions. That is to say, the misfit between either the Th or U distribution and log-normal distributions with the same μ and σ is negligible according to the (admittedly simplistic) statistical test mentioned above. On the other hand, the misfit between Th or U and the corresponding gamma distributions with the same shape and rate parameters is significant according to the same statistical test. Th and U are expected to be skewed because their abundance changes rapidly as a function of depth (e.g., Rudnick & Fountain, 1995; Huang et al., 2013; Rudnick & Gao, 2014).

7 A Basalt, by Any Other Name

If the deep (particularly the lower) continental crust looks like granulite facies xenoliths, or to an extent amphibolite facies lithologies, then it looks like a basalt. Similarities between these deep crustal samples and mid ocean ridge basalt (MORB) and ocean island basalt (OIB) span SiO_2, Al_2O_3, MgO, and MnO (Fig. 7, Table 2). CaO and Na_2O differ by about 10% among the three different basalts, with MORBs having the highest concentration of both. An important note, though, is that all of our deep crustal analogues are depleted in Ti compared to MORB or OIB. Since there is no complementary Ti enrichment in the upper crust (e.g., Taylor & McLennan, 1985; Wedepohl, 1995; Rudnick & Gao, 2014), there may exist an unsampled Ti reservoir on Earth (McDonough, 1991; Rudnick et al., 2000).

If the deep crust resembles granulite facies terrains, then it differs more substantially from MORB and OIB (Fig. 8). Granulite facies terrains have 16-27% higher SiO_2 content than MORB and 3 to 4 times higher concentrations of incompatible elements as a result. However, while comparable in major element space, both granulite facies xenoliths and terrains have on average $\frac{1}{3}$ to $\frac{1}{2}$ the concentration of LREEs of OIBs. The undepleted or otherwise uniquely enriched source of OIB material is not reflected in crustal basalts.

Eclogite facies lithologies are essentially basaltic in their bulk compositions and comparable to that of MORBs & OIBs (Table 2) when normalized to 100 wt.%. With 16 wt.% Al_2O_3, 9 wt.% FeO_T, and varying amounts of MgO, however, we expect eclogite facies

lithologies to maintain their traditionally-higher-than-basaltic densities. Differences in expected deep crustal densities, discussed below, suggest that eclogites will by and large be gravitationally unstable in most lower crustal models.

8 Constructing the Continental Crust

The composition of the deep continental crust is a direct result of the many processes through which it was constructed and evolved. The abundance of incompatible elements in our dataset provides a tool for analyzing the probability of different deep crustal compositions. Figure 9 shows the abundance of incompatible elements for the different lithologies plotted as a function of their normalized abundances. This order of elements changes for each lithology, with the overall order approximating an element's relative incompatibility during intra-crustal differentiation. Overall, few differences in the order of elements are observed between each panel. Noteworthy, the absolute abundances correlate with how chemically evolved the lithology is, with higher SiO_2 compositions having higher concentrations of the highly incompatible elements. Also of significance, uncertainties decrease with increasing compatibility, with some strong exceptions in our more limited datasets (e.g., eclogite facies terrains). Unsurprisingly, Al_2O_3 has the lowest uncertainty.

Figure 9 documents the elements that change their relative compatibility between different lithologies. In particular, Th shows high variability in its relative position. While granulite facies xenoliths are depleted in both Th and U, they are relatively more depleted in Th, as are eclogite facies terrains. Eclogite facies lithologies on the whole are depleted in both Th and U compared to other incompatible elements - unsurprising given their mafic compositions and limited mineralogies. In all of these lithologies U, Th, and other highly incompatible elements are concentrated in accessory phases, such as zircon, apatite, and titanite, and the stability of these phases control the distribution of these elements in the crust. In all lithologies, except Archean granulite facies terrains, U is more incompatible than Th, which in principle should lead to lower Th/U values. However, on average (as shown above) these lithologies have κ_{Pb} values approximately equal to the bulk Earth's value.

Using a simplified, 3-layer modeling approach, we identify the elements that stand out as markers of different crustal compositions and formation processes, and which contribute significantly to estimates of bulk silicate Earth (BSE) composition. Our bulk continental crust composition is calculated by weighting the elemental abundances from the upper, middle, and lower crust by each layer's mass fraction (Table 3). The mass fractions of these crustal layers are from Wipperfurth et al. (2020). The upper crust's composition uses Gaschnig et al. (2016)'s concentrations for all elements for the top $\frac{1}{3}$ except Sr and Mo (Rudnick & Gao, 2014), and Rudnick and Gao (2014) for the bottom $\frac{2}{3}$ of the upper crust. We take the upper crust HSEs from (Chen et al., 2016), and Ag from (Chen et al., 2020). We use amphibolite facies lithologies as representatives of a middle crustal composition and split the lower crust 50/50 between granulite facies xenoliths and terrains. Debate remains regarding models for the composition of the lower crust (e.g., Rudnick & Gao, 2014; Hacker et al., 2015); there is no obvious Gordian Knot solution to determining the composition of the lower crust. Our solution for deciding on a model for the lower crust's composition recognizes that granulite facies terrains come from on average ∼0.8 GPa (Brown & Johnson, 2019), approximately the upper portion of the lower crust, whereas granulite facies xenoliths appear to dominate he bottom of the lower crust (Rudnick & Gao, 2014).

Though amphibolite facies lithologies are held to represent the middle crust, the median SiO_2 for amphibolite lithologies is ∼10% lower than existing estimates. This makes our bulk continental crustal model more mafic in the middle crust, leaving a potential

mid-crustal deficit in many incompatible elements. A mafic bias in our amphibolite facies lithologies may exist and seems to stem from:

1) biasedly assigning medium grade mafic metamorphic samples to the amphibolite facies (due to the hallmark abundance of amphiboles) but not assigning medium grade felsic metamorphics to the amphibolite facies; and

2) the oversampling of mafic amphibolite facies locations.

Figures 9 and 10 order elements, from left to right, from the most to least abundant in the continental crust, relative to a BSE model. In doing so, we highlight the enrichments of Cs, Rb, Ba, Pb, U, Th, K, W, and La in the continental crust and identify the crust as an important host for these elements in the bulk silicate Earth (BSE), despite its insignificant mass contribution (0.55% of the BSE mass). Assuming a BSE composition (McDonough & Sun, 1995; Palme & O'Neill, 2014), the estimated crustal contribution represents 15 to 50% of Earth's total budget of these elements sequestered in the continental crust. Importantly, ∼35% of the heat producing elements are stored in the crust and not available for driving mantle convention.

The continental crust is often viewed as the complementary reservoir of the Depleted Mantle, particularly for the incompatible elements. In Figure 10 we compare the composition of the continental crust with that of the average MORB, a representation for the upper portion of the oceanic crust. A crude comparison of the composition of the Depleted Mantle (DM) can be taken as $\sim \frac{1}{10}$ the value of MORB. If the upper mantle (mantle above the 670 km seismic discontinuity; 26% of the mass of the BSE), often considered the Depleted Mantle, was uniformly depleted to create the continents, then it cannot be the complement to the continental crust. Elements whose crustal mass contribution exceeds 26% (i.e., Cs, Rb, Ba, Pb, U, Th, K, and W) require that the lower mantle has been accessed during the production of continental crust. Therefore, the part of the BSE referred to as the Depleted Mantle extends considerably into the lower mantle (nearly half a mantle mass is necessary to account for all of the Rb & Cs in the continental crust). The implications of this finding demand that all or most of the mantle has been involved, to some extent, in the production of the continents.

Apparent non-complementary relationships are found for K, Sr, and Li. The average MORB (Gale et al., 2013) pattern (Figure 10) shows marked depletion in the primitive mantle normalized abundance for K, Sr, and Li relative to adjacent elements. The relative incompatibility of these elements during mantle melting are K∼U, Sr∼Pr-Nd, and Li∼Dy (Sun & McDonough, 1989). The K/U values of continental crust and MORB are complementary relative to that of the BSE (Arevalo et al., 2009; Farcy et al., 2020), consistent with these patterns (Figure 10). The marked depletion in Sr seen in the MORB pattern is due to these basalts having experienced considerable plagioclase fractionation. However, as Tang et al. (2017) noted, MORBs with ⩾10wt.% MgO, primitive MORBs that have yet to experience plagioclase fractionation, do not show any depletion in Sr. Finally, the depletion in Li is somewhat more challenging to explain. Lithium's position (established by crustal abundances) suggests its relative incompatibility is enhanced due, most likely, to a combination of melting and weathering processes. That said, however, the continental crust, which hosts only ∼6% of the BSE's Li budget, cannot account for the marked depletion seen in the MORB pattern. (Moving the MORB Li data point over to the heavy REE still does not account for its depletion.) We offer no explanation for this enigmatic observation.

Another method to determine deep crustal lithology is to test its composition with seismic (Christensen & Mooney, 1995; Rudnick & Fountain, 1995) and gravity data. Seismic velocities and densities are controlled by mineral forming, major elements (e.g., SiO_2 and CaO), not the highly incompatibles. However, highly incompatibles correlate to a sample's degree of differentiation (i.e., SiO_2 content); therefore, incompatible element abundances can still be derived from major element concentrations. Table 4 compares

the continent's expected velocities and densities for the middle (MC) and lower (LC) crust based on different geophysical and geochemical models. Our MC model has a middle crust of Vp = 6.8 km/s, Vs = 4.0 km/s, and density of 2980 kg/m^3, values higher than other models. A middle crust calculated from Rudnick and Gao (2014)'s average composition also has a high density (Brocher, 2005) when compared to the Vp and surface wave predictions of CRUST 1.0 (Laske et al., 2016) and LITHO 1.0 (Pasyanos et al., 2014). These inconsistencies between geochemical and geophysical predictions extend into the deep crust, again with all but the lowest density and Vp geochemical estimates (Hacker et al., 2015) exceeding seismic expectations. Though these global averaged seismic models are not infallible, a reconciliation is still required between the geochemical based and geophysical based models for Earth's deep crust.

9 Conclusion

The deep continental crust will remain a topic of intense debate for years to come due to its inaccessibility. Amphibolite, granulite, and eclogite facies metamorphic terrains and xenoliths serve as our windows to middle and lower continental crust. Compositional variability even within these facies underscores the potential for deep crustal heterogeneity, though certain elements and patterns anchor our understanding of the chemistry of the crust. The Daly Gap, evident in amphibolite facies lithologies and granulite facies terrains, dominates the relative abundance of SiO_2 in the deep crust, especially its lowermost portions. The more homogeneous mineralogy of eclogite facies lithologies distinguishes them from amphibolite or granulite facies lithologies, though all three could plausibly contribute to previous deep crustal compositional estimates. Constraining the proportion of mafic to felsic material in the deep crust will in turn constrain its trace element content and distribution, because its enrichment or depletion in these elements is most heavily influenced by differentiation processes.

Thankfully, all is not lost when using these samples to parse out the composition of the deep crust. The amount of Al_2O_3 is similar among all of the samples, as are the heavy rare earth elements. We find that the concentrations of Er, Tm, Yb, and Lu in particular show little variation among samples of different metamorphic grades. The controlling factor in incompatible element abundance among our deep crustal lithologies is how differentiated the material is, not metamorphic grade. This means that igneous processes and protolith composition rather than metamorphic processes dictate the chemical signatures of the deep crust.

Although the deep continental crust has been studied at length, many elements still lack sufficient concentration data (such as the highly siderophile elements). Future studies will be challenged to reduce the size of the uncertainty on element concentrations, and since instrumental precision is not the main source of uncertainty, inquiry into the processes that alter elemental abundances in different samples will have to be identified and explained. As it stands, there is also a density discrepancy between highly cited geochemical models (e.g. Rudnick and Gao (2014) versus Hacker et al. (2015)) and common geophysical crust models, with geochemical samples suggesting a deep crust that has higher overall density than what is seismically observed. Ultimately, the future of deep crustal modeling will depend on the integration of multiple types of datasets, such as geochemical and seismological measurements and gravity analyses.

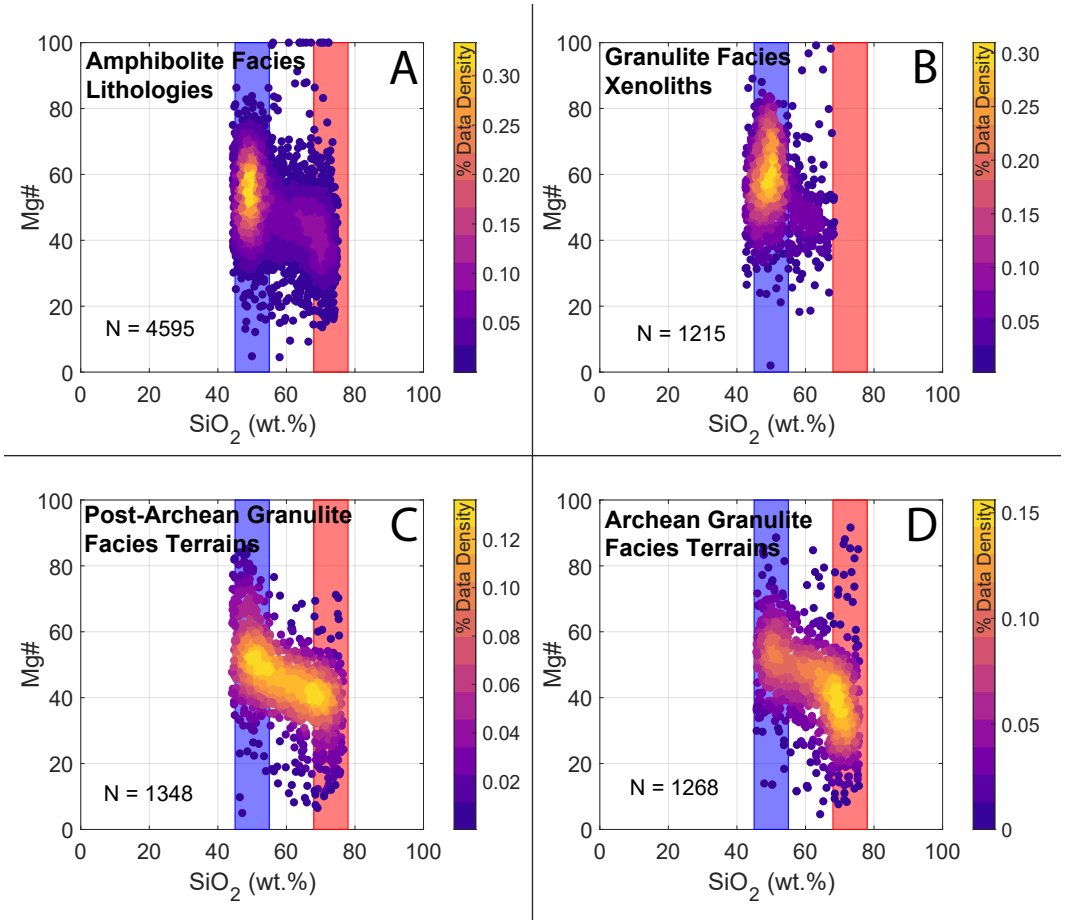

Figure 1. Mg# vs. SiO_2 for A) amphibolite lithologies, and granulite facies B) xenoliths, C) Post-Archean terrains, and D) Archean terrains. Color indicates relative data point density. Blue and red fields mark mafic and felsic SiO_2 abundances. Mg # is calculated as molar $\frac{[Mg]}{[Mg]+[Fe]}$. All show high concentrations of mafic and/or felsic compositions and comparatively few compositions of intermediate SiO_2.

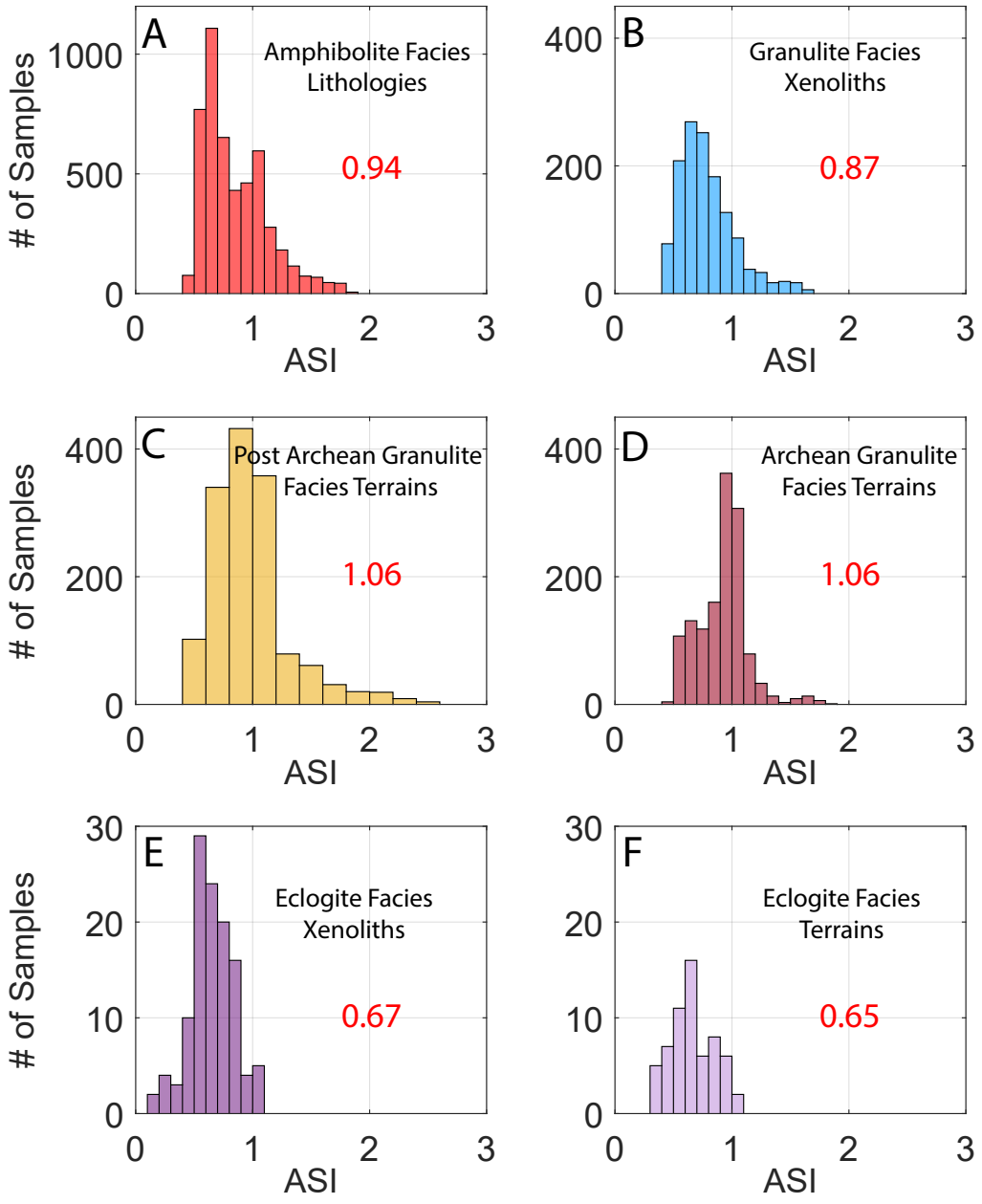

Figure 2. Natural log of the aluminum saturation index index (ASI), molar $Al_2O_3/(CaO + Na_2O + K_2O)$. Red numbers indicate the median value for each sample type. The ASI value is an ambiguous indicator of a rock's protolith; rocks with ASI >1 can be from igneous or metasedimentary protoliths

can be an indicator of metasedimentary contributions to sample populations since sediments are typically more Al rich than igneous sources. The more mafic datasets have smaller ASI values while the granulite facies terrains can more often have values around 1.

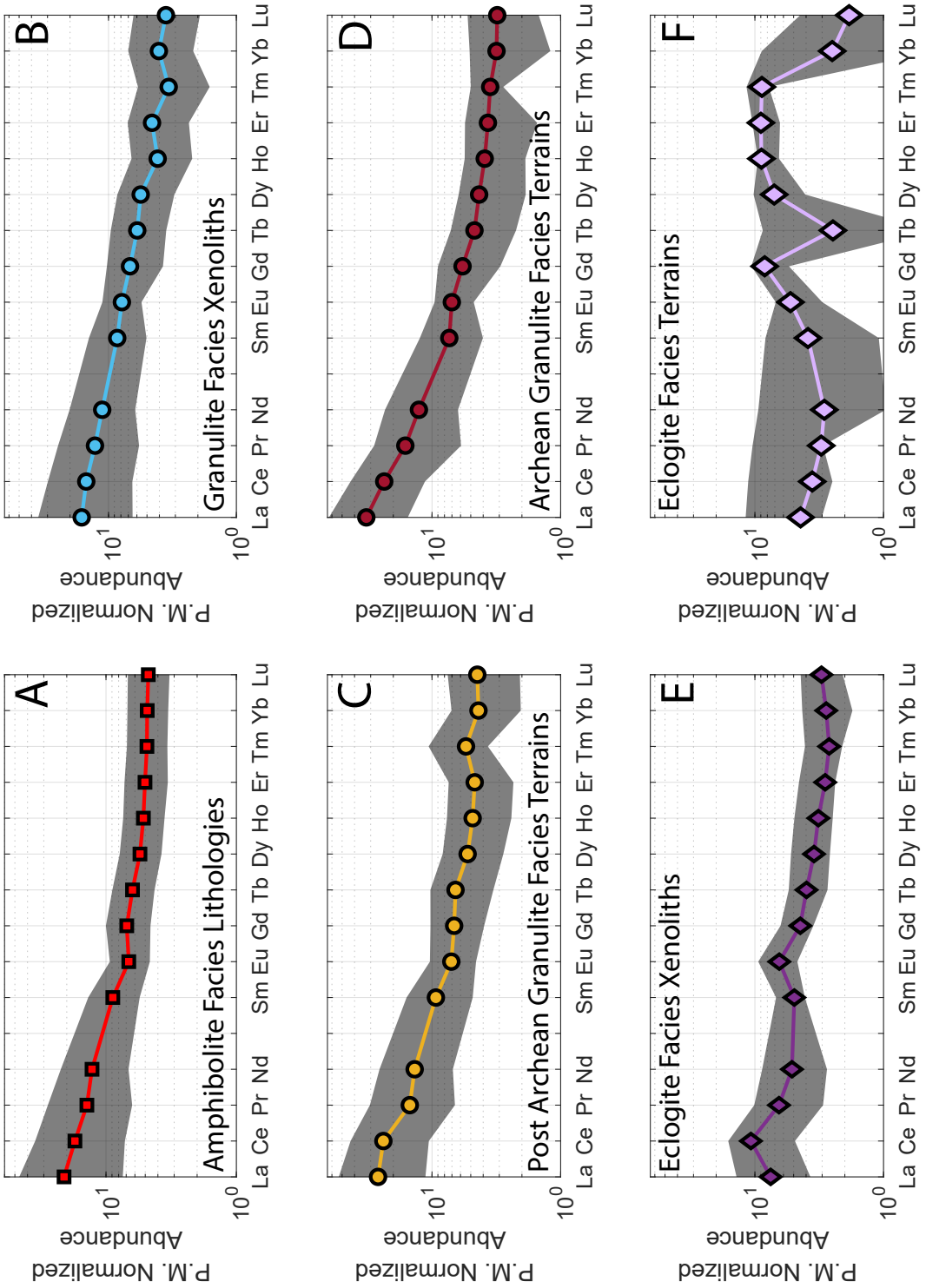

Figure 3. Rare earth element median values. The gray shaded bands represent the 1st and 3rd quartile values for each REE.

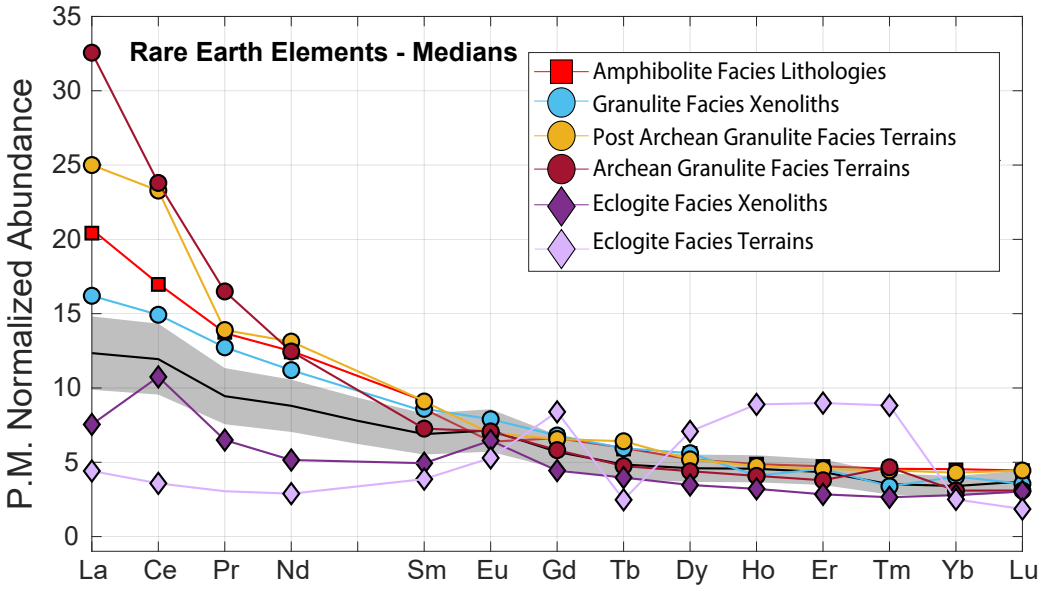

Figure 4. While the most variation is seen in the light rare earth elements, the heavy rare earth elements are tightly knit around 0.25 ppm (5x primitive mantle). Note the linear scale. The black line and gray shaded region surrounding it is the Rudnick and Gao (2014) lower crustal composition ± 15%.

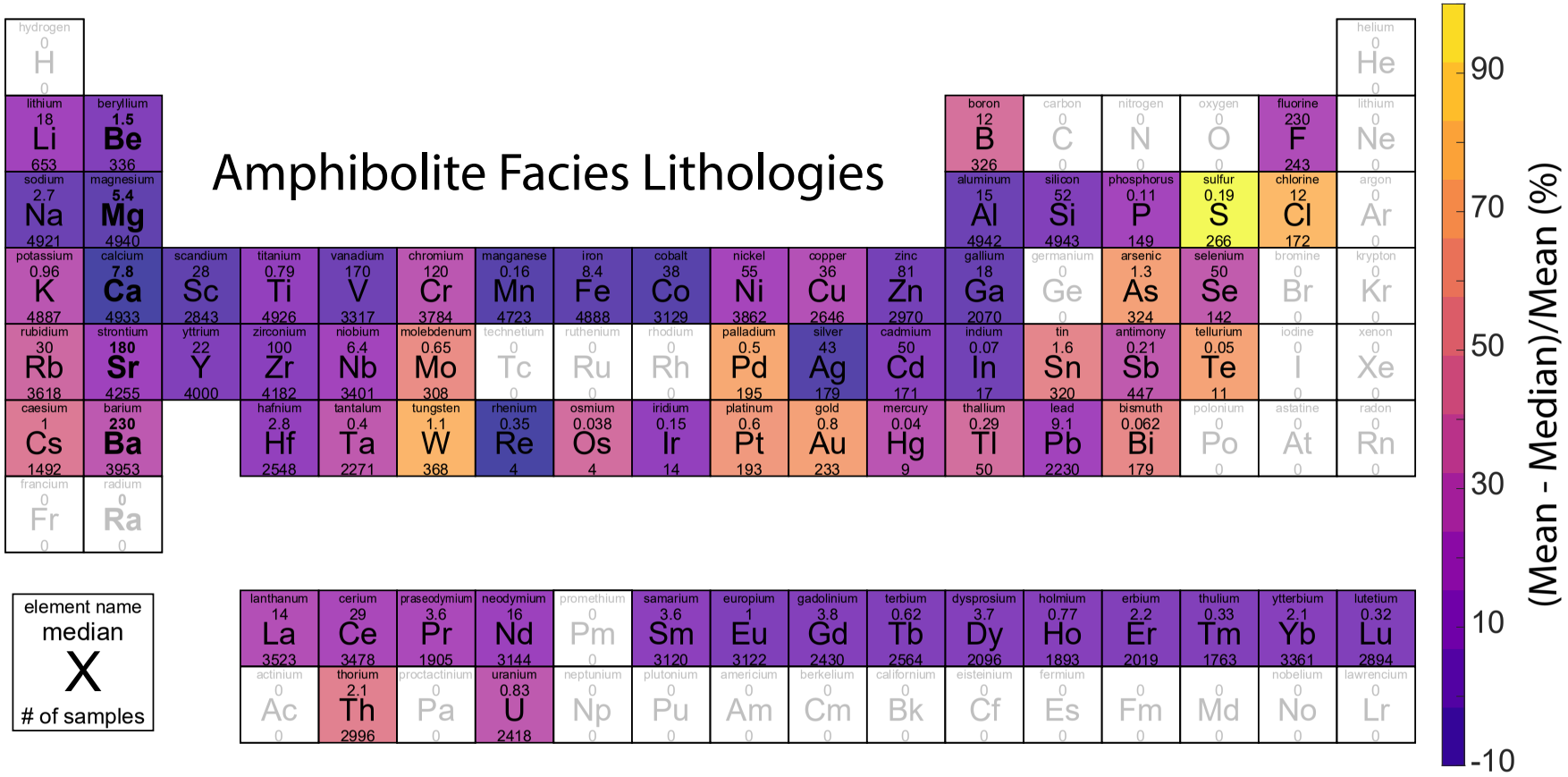

Figure 5. The percent difference between the mean and median for elemental distributions is an indicator of the symmetry of the distribution. On this periodic table, color correlates to that percent difference. Elements that are grayed out have insufficient data. The number at the bottom of each element box is the number of available samples, and the top number is the median concentration. Median concentrations are given in wt.% oxide for Na, Mg, Al, Si, K, Ca, Ti, Mn, and Fe. All other elements are reported in ppm. Similar trends emerge among elements of the same family and among the lathanides. Heavier, larger elements vary more in amphibolite facies lithologies than in granulite facies lithologies.

manuscript submitted to *Geochemistry, Geophysics, Geosystems*

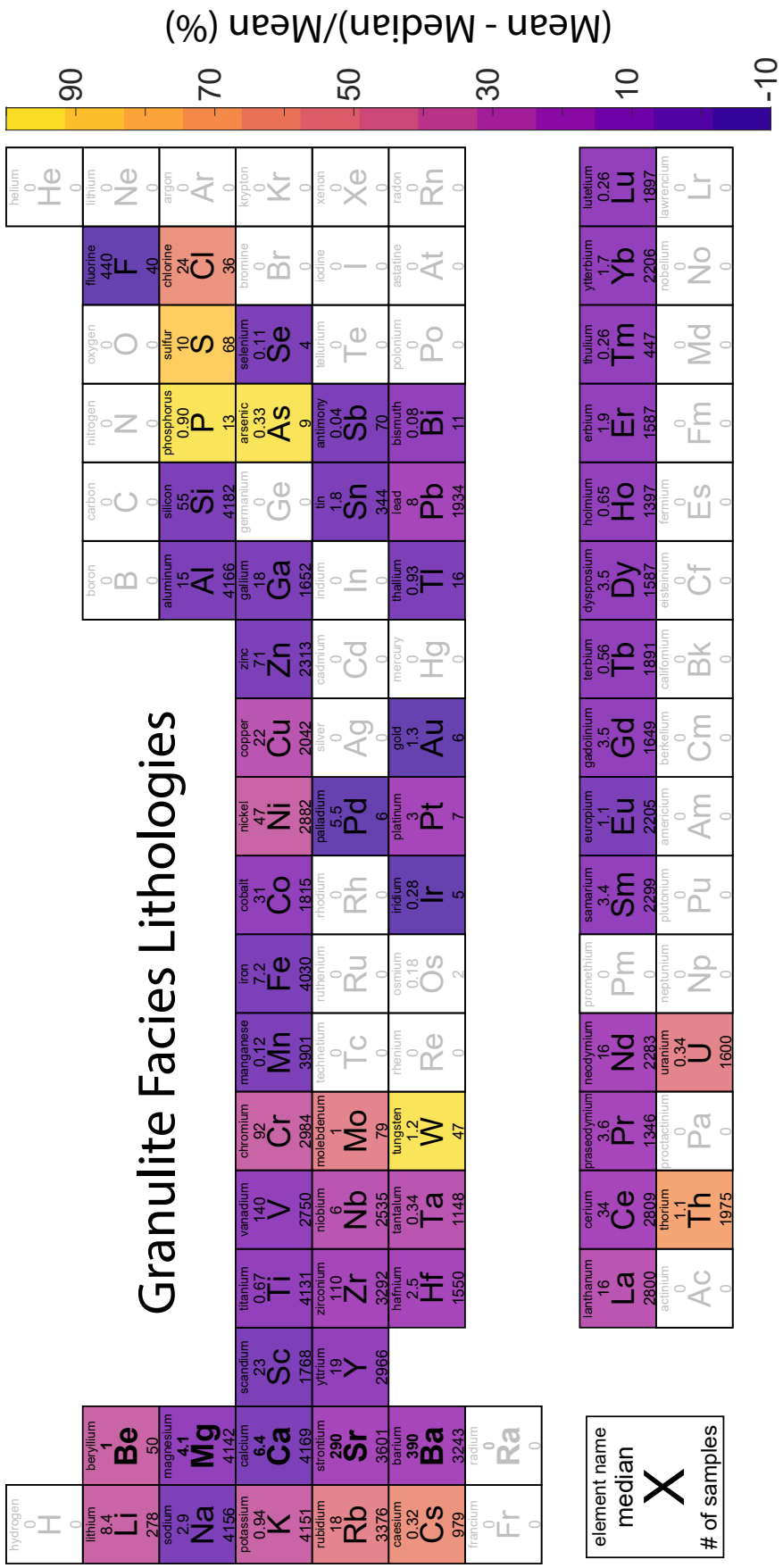

Figure 6. Color correlates to the percent difference between the mean and median concentration of a given element in granulite facies lithologies. Elements that are grayed out have insufficient data. The number at the bottom of each element box is the number of available samples, and the top number is the median concentration. Median concentrations are given in wt.% oxide for Na, Mg, Al, Si, K, Ca, Ti, Mn, and Fe. All other elements are reported in ppm. Terrains and xenoliths are treated as one dataset since there is no observable difference between terrains and xenoliths of comparable SiO_2. As with amphibolite facies lithologies, Al and Ga are the narrowest, least variable distributions. Similar trends emerge among elements of the same family and among the lathanides.

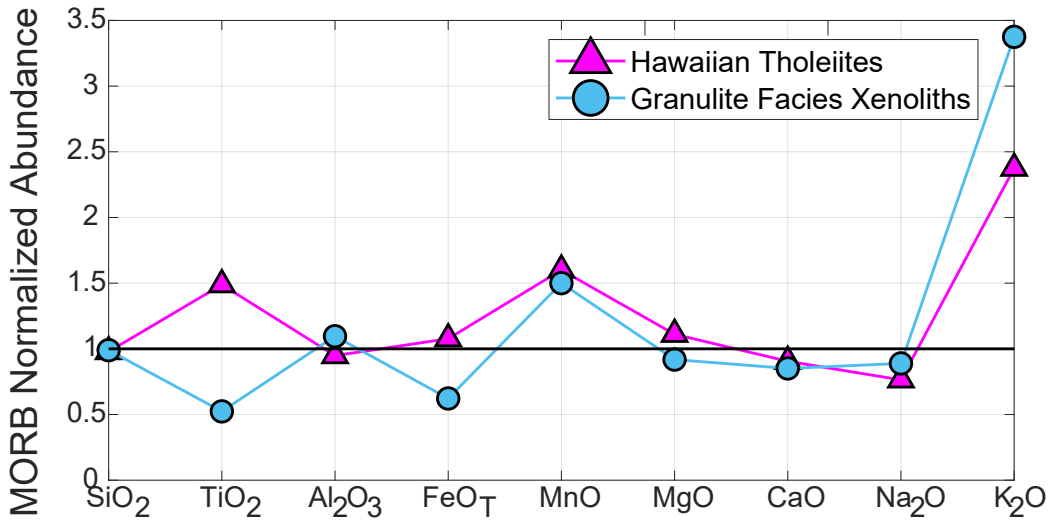

Figure 7. Ocean island basalt Hawaiian tholeiites (MacDonald & Katsura, 1964) and granulite facies xenoliths have similar major element patterns except in TiO_2. Both resemble mid ocean ridge basalts (Gale et al., 2013) except in TiO_2 and K_2O.

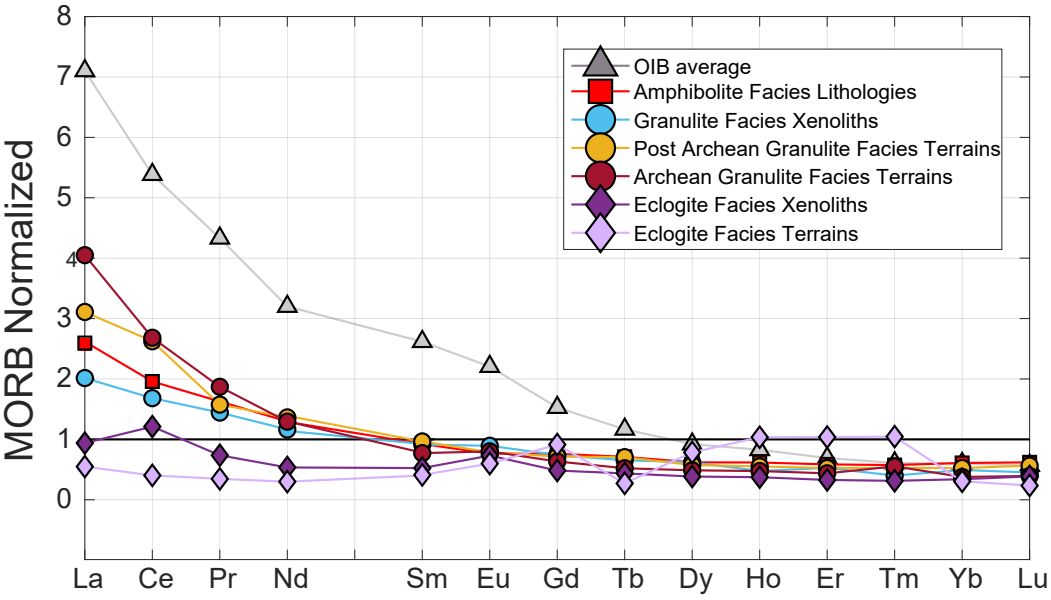

Figure 8. Rare earth element concentrations for granulite and amphibolite facies lithologies fall between MORB (Gale et al., 2013) and OIB (Arevalo & McDonough, 2010) abundances. The shape of their REE patterns, however, resemble OIB moreso than MORB. Amphibolite, granulite, eclogite, and OIB rare earth element patterns converge towards the heavy rare earths.

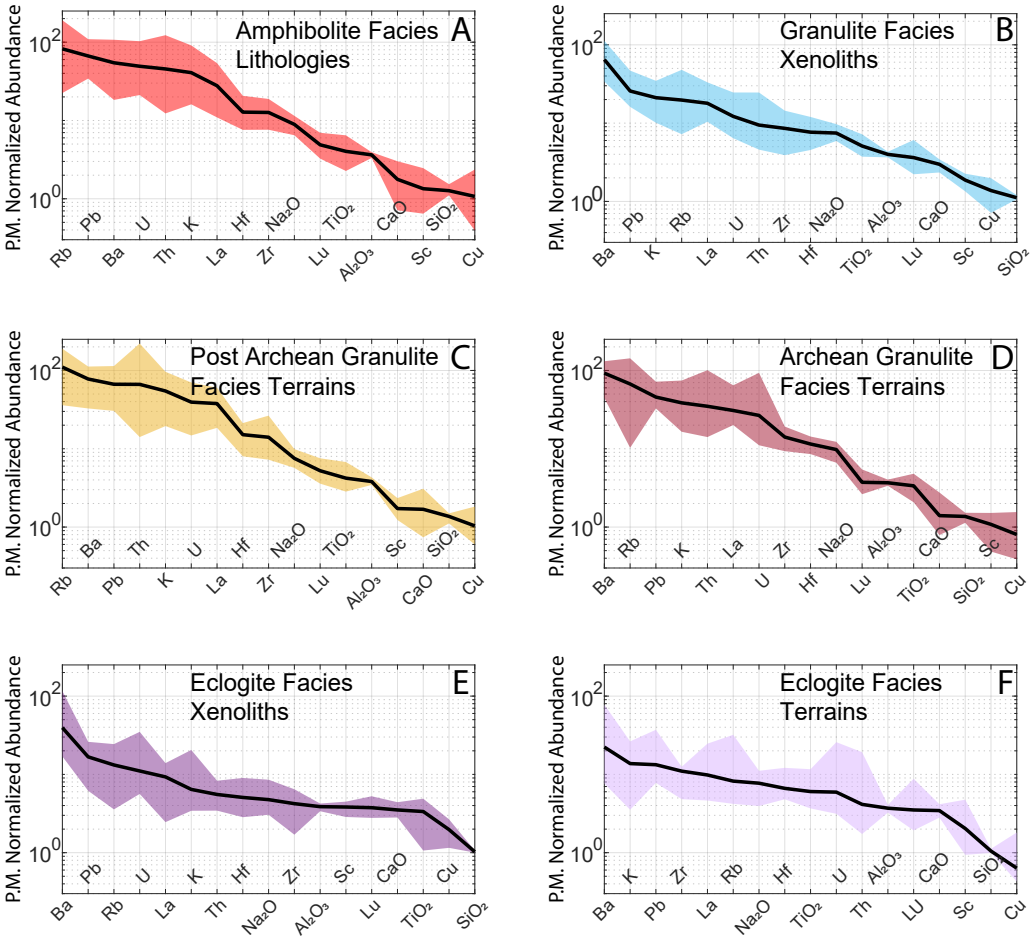

Figure 9. Incompatible element abundances for amphibolite, granulite, and eclogite facies lithologies normalized to primitive mantle values (McDonough & Sun, 1995). Element compatibility increases from left to right. Elements are ordered from left to right on the by relative enrichment in the continental crust, therefore elements change order on the x-axis in different panels.

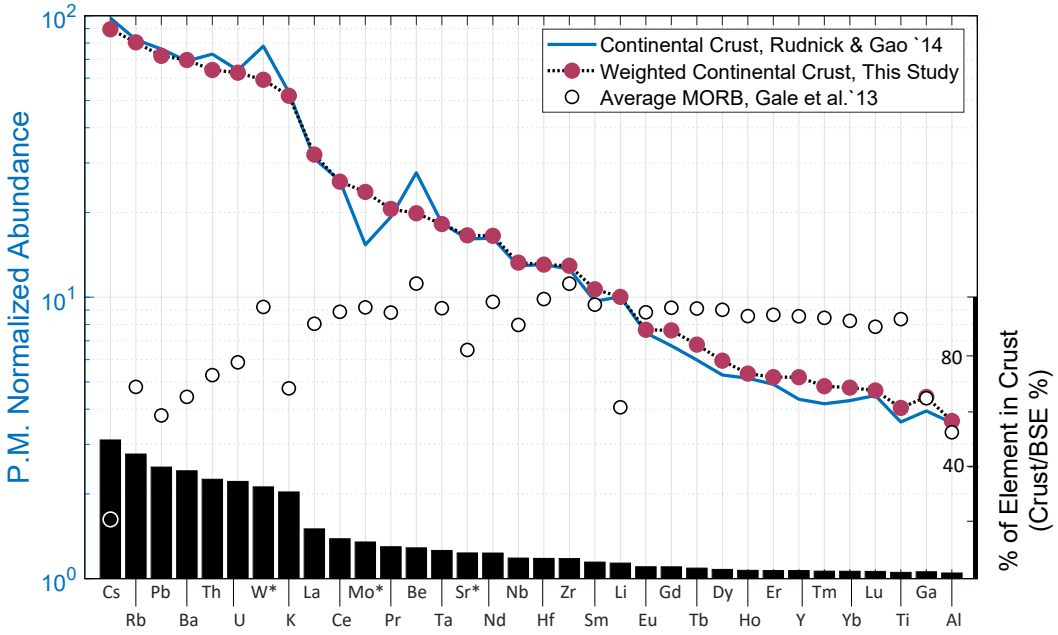

Figure 10. THIS IS A PLACEHOLDER FIGURE WITH UGLY COLORS Weighted proportions of amphibolite and granulite facies lithologies were combined with upper crustal values (see text) to generate bulk silicate Earth incompatible element abundance estimates. Elements are ordered from left to right by relative enrichment in the continental crust. Alternatively, this ordering reflects element compatibility during mantle melting. Colored circles show our bulk continental crust model while empty circles plot MORB abundances. Black bars follow the right-hand y-axis and show the % of each element sequestered in the continental crust relative to BSE. Normalized to (McDonough & Sun, 1995) with W from (Arevalo & McDonough, 2008).

764 STD - standard deviation
765 IQR - interquartile range
766 Geo-Mean - geometric mean
767 Geo-STD - geometric standard deviation (reported in log units)
768 γ - gamma function mean, $\kappa * \sigma$ (scale parameter $*$ shape parameter)
769 $\gamma - STD$ - gamma function standard deviation, $\sqrt{\kappa * \sigma^2}$

Table 1: Major Element Compositions

	Mean	Median	Geo-Mean	γ-Mean	STD	IQR	Geo-STD	γ-STD	N (filtered)	N (original)
	Amphibolite Facies Lithologies									
SiO_2	59.1	57.1	58.4	59.1	9.43	18.2	1.17	9.37	2240	5490
TiO_2	0.830	0.730	0.684	0.830	0.494	0.653	1.92	0.50	2240	5490
Al_2O_3	14.8	14.8	14.7	14.8	1.57	2.15	1.11	1.58	2240	5490
FeO_T	5.31	5.26	4.33	5.31	2.88	5.03	2.03	3.29	847	2510
MnO	0.130	0.138	0.111	0.130	0.0650	0.120	1.85	0.07	2220	5430
MgO	4.13	3.70	2.93	4.13	2.81	5.03	2.57	3.27	2240	5490
CaO	5.94	5.69	4.58	5.94	3.61	6.95	2.23	4.13	2230	5480
Na_2O	2.96	2.97	2.78	2.96	0.985	1.46	1.46	1.06	2230	5480
K_2O	1.72	1.32	1.18	1.72	1.33	2.05	2.60	1.42	2230	5470
P_2O_5	0.148	0.138	0.125	0.148	0.0830	0.110	1.84	0.0840	2157	5284
Mg#	46.4	46.8	45.0	46.4	10.6	15.1	1.28	11.2	2220	5430
	Granulite Facies Xenoliths									
SiO_2	51.6	50.2	51.3	51.6	5.05	4.96	1.10	4.88	147	1490
TiO_2	0.975	0.923	0.879	0.975	0.415	0.581	1.62	0.436	144	1480
Al_2O_3	16.20	16.20	16.10	16.20	1.74	2.31	1.11	1.75	147	1490
FeO_T	6.76	6.71	6.42	6.76	2.15	2.75	1.39	2.16	81	723
MnO	0.150	0.147	0.143	0.150	0.0431	0.0563	1.36	0.0446	143	1440
MgO	7.05	7.19	6.60	7.05	2.29	3.14	1.48	2.55	145	1480
CaO	9.23	9.56	8.83	9.23	2.48	3.27	1.37	2.73	147	1490
Na_2O	2.56	2.48	2.44	2.56	0.744	1.14	1.38	0.783	147	1490
K_2O	0.779	0.658	0.604	0.779	0.543	0.716	2.10	0.535	147	1480
P_2O_5	0.163	0.153	0.130	0.163	0.101	0.132	2.08	0.106	143	1434
Mg#	56.9	57.1	56.2	56.9	9.05	12.9	1.18	9.16	145	1480
	Post Archean Granulite Facies Terrains									
SiO_2	59.3	61.5	58.6	59.3	8.73	16.10	1.16	8.83	145	1660
TiO_2	0.871	0.763	0.752	0.871	0.438	0.650	1.78	0.462	122	1630
Al_2O_3	15.8	15.5	15.6	15.8	2.05	2.88	1.14	2.04	122	1630
FeO_T	5.75	5.59	5.33	5.75	2.10	3.33	1.50	2.21	81	758
MnO	0.129	0.130	0.120	0.129	0.0447	0.0711	1.50	0.0487	120	1600
MgO	5.06	4.10	3.79	5.06	3.64	5.06	2.25	3.70	123	1630
CaO	6.11	5.41	4.83	6.11	3.76	7.17	2.08	4.05	123	1630
Na_2O	2.51	2.50	2.33	2.51	0.860	1.32	1.51	0.954	122	1620
K_2O	1.87	1.73	1.30	1.87	1.36	2.09	2.66	1.53	155	1700
P_2O_5	0.150	0.122	0.119	0.150	0.100	0.111	2.05	0.100	112	1454
Mg#	48.0	45.8	46.5	48.0	12.0	15.7	1.28	11.9	119	1610
	Archean Granulite Facies Terrains									
SiO_2	60.1	61.5	59.5	60.1	8.44	16.9	1.15	8.52	123	1530
TiO_2	0.655	0.609	0.575	0.655	0.338	0.422	1.68	0.327	122	1490
Al_2O_3	15.3	14.9	15.2	15.3	2.10	2.36	1.14	2.02	122	1510
FeO_T	5.12	4.13	4.06	5.12	3.28	5.08	2.05	3.37	78	902

MnO	0.117	0.101	0.101	0.117	0.0607	0.0940	1.79	0.0633	112	1440
MgO	4.36	3.72	3.40	4.36	2.88	4.53	2.10	2.96	123	1520
CaO	5.33	4.49	4.25	5.33	3.24	5.65	2.08	3.48	122	1510
Na_2O	3.05	3.24	2.83	3.05	1.06	1.63	1.51	1.17	120	1500
K_2O	1.50	1.20	1.14	1.50	1.06	1.67	2.18	1.07	125	1630
P_2O_5	0.163	0.156	0.144	0.163	0.0815	0.0870	1.67	0.0795	105	1426
Mg#	48.3	47.0	47.3	48.3	9.81	12.2	1.22	9.56	122	1500
	Eclogite Facies Xenoliths									
SiO_2	46.2	46.2	46.1	46.2	1.91	2.46	1.04	1.93	15	173
TiO_2	0.617	0.607	0.490	0.617	0.344	0.621	2.15	0.406	15	173
Al_2O_3	16.1	15.7	15.9	16.1	2.79	2.76	1.17	2.61	15	173
FeO_T	8.56	8.74	8.39	8.56	1.64	2.63	1.23	1.72	6	46
MnO	0.186	0.176	0.183	0.186	0.0368	0.0347	1.20	0.0342	15	172
MgO	11.7	11.6	11.3	11.7	3.02	4.34	1.31	3.07	15	173
CaO	11.4	11.3	11.1	11.4	2.49	4.99	1.26	2.55	15	173
Na_2O	2.06	1.58	1.61	2.06	1.49	1.31	2.06	1.39	15	173
K_2O	0.375	0.200	0.211	0.375	0.404	0.380	3.09	0.374	14	131
P_2O_5	0.0652	0.0631	0.0550	0.0652	0.0295	0.0353	1.97	0.0371	12	86
Mg#	51.8	47.9	50.8	51.8	9.90	15.20	1.21	9.71	13	123
	Eclogite Facies Terrains									
SiO_2	47.5	47.2	47.4	47.5	2.64	5.33	1.06	2.65	14	60
TiO_2	1.33	1.09	1.14	1.33	0.715	1.23	1.79	0.732	14	60
Al_2O_3	14.9	15.0	14.8	14.9	2.14	3.26	1.16	2.16	14	60
FeO_T	9.06	8.59	8.48	9.06	3.27	6.30	1.44	3.27	11	31
MnO	0.227	0.192	0.212	0.227	0.0894	0.115	1.41	0.0804	14	60
MgO	8.11	7.98	7.80	8.11	2.42	2.80	1.31	2.25	14	60
CaO	11.1	11.1	10.9	11.1	2.13	3.85	1.22	2.18	14	60
Na_2O	2.74	2.56	2.36	2.74	1.57	2.25	1.72	1.46	14	59
K_2O	0.454	0.428	0.314	0.454	0.334	0.691	2.54	0.371	12	57
P_2O_5	0.134	0.108	0.097	0.134	0.106	0.117	2.27	0.102	14	57
Mg#	41.7	40.8	40.8	41.7	8.84	9.60	1.24	8.95	14	60

Table 2. Median major oxide compositions for our sample sets, mid ocean ridge basalts (MORB, (Gale et al., 2013)), and ocean island basalts (OIB, (MacDonald & Katsura, 1964))

	Amph. Lith.	Gran. Xen.	PA Gran. Ter.	A Gran. Ter.	Ecg. Xen.	Ecg. Ter.	MORB	OIB
SiO_2	57.1	50.2	61.5	61.5	46.2	47.2	50.5	49.4
TiO_2	0.730	0.923	0.763	0.609	0.607	1.09	1.68	2.50
Al_2O_3	14.8	16.2	15.5	14.9	15.7	15.0	14.7	13.9
FeO_T	5.26	6.71	5.59	4.13	8.74	8.59	10.4	11.2
MnO	0.138	0.147	0.130	0.101	0.176	0.192	0.184	0.160
MgO	3.70	7.19	4.10	3.72	11.60	7.98	7.58	8.42
CaO	5.69	9.56	5.41	4.49	11.3	11.1	11.4	10.3
Na_2O	2.97	2.48	2.50	3.24	1.58	2.56	2.79	2.13
K_2O	1.32	0.658	1.73	1.20	0.200	0.428	0.160	0.380
P_2O_5	0.138	0.153	0.122	0.156	0.0631	0.108	0.184	0.245
Mg#	46.8	57.1	45.8	47.0	47.9	40.8	-	-
Mg# Calc.	55.6	65.6	56.7	61.6	70.3	62.3	56.4	57.2

Table 3: Recommended Continental Crust Composition

	Upper Crust	Middle Crust	Lower Crust	Deep Crust	Bulk Crust
SiO_2	68.0	62.2	53.3	57.6	61.1
TiO_2	0.663	0.795	0.980	0.889	0.812
Al_2O_3	15.1	16.1	17.2	16.66	16.1
FeO_T	5.21	5.73	7.12	6.44	6.02
MnO	0.100	0.150	0.156	0.153	0.135
MgO	2.29	4.03	7.63	5.87	4.66
CaO	2.75	6.20	10.15	8.21	6.36
Na_2O	2.63	3.23	2.63	2.93	2.82
K_2O	3.11	1.44	0.698	1.06	1.75
P_2O_5	0.169	0.150	0.162	0.156	0.161
Li	26.8	15.0	6.89	10.9	16.0
Be	2.18	1.44	0.478	0.956	1.35
B	10.6	9.00	-	-	-
N	51.1	-	-	-	-
F	343	399	-	-	-
S	382	22.0	140	81	178
Cl**	181	29.3	151	90.5	120
Sc	13.3	21.0	28.0	24.5	20.9
V	88.1	134	186	160	137
Cr	77.2	81.0	168	125	109
Co	15.2	29.9	46.8	38.4	30.9
Ni	39.2	39.7	100	70.1	60.1
Cu	26.3	30.0	37.8	33.9	31.5
Zn	69.3	78.0	81.1	79.6	76.2
Ga	17.8	18.0	17.3	17.6	17.7
Ge	1.53	-	-	-	-
As	2.92	1.30	-	-	-
Se	0.058	0.0530	-	-	-
Br	0.98	-	-	-	-

Rb	92.8	43.8	10.6	27.1	48.3
Sr†	320	201	465	334	329
Y	25.7	22.5	19.0	20.7	22.3
Zr	203	123	83.3	103	135
Nb	12.1	7.20	7.00	7.10	8.73
Mo†**	1.12	0.520	1.90	1.21	1.18
Ru	0.240	-	-	-	-
Rh	-	-	-	-	-
Pd**	0.000800	0.000850	0.00554	0.00321	0.00214
Ag†	0.0329	0.0480	-	-	-
Cd	0.097	0.0600	-	-	-
In	0.058	0.0710	-	-	-
Sn	2.23	1.60	1.58	1.59	1.80
Sb	0.39	0.200	-	-	-
Te	-	0.0500	-	-	-
I	0.862	-	-	-	-
Cs	4.18	1.19	0.390	0.787	1.88
Ba	665	330	393	362	460
La	33.3	18.1	11.6	14.8	20.8
Ce	67.0	36.5	27.0	31.7	43.1
Pr	7.65	4.68	3.48	4.08	5.23
Nd	29.4	18.3	14.7	16.5	20.7
Sm	5.38	4.10	3.57	3.83	4.33
Eu	1.15	1.09	1.29	1.19	1.18
Gd	4.79	3.91	3.77	3.84	4.15
Tb	0.780	0.664	0.570	0.618	0.670
Dy	4.55	3.91	3.60	3.75	4.01
Ho	0.95	0.822	0.640	0.730	0.800
Er	2.67	2.29	1.89	2.09	2.28
Tm	0.380	0.350	0.254	0.302	0.327
Yb	2.44	2.19	1.70	1.94	2.10
Lu	0.370	0.330	0.245	0.287	0.315
Hf	5.73	3.42	2.05	2.73	3.70
Ta	0.900	0.540	0.597	0.569	0.677
W†◇**	1.59	0.440	0.310	0.374	0.773
Re†	0.000220	-	-	-	-
Os†**	0.0000418	-	0.0000210	-	-
Ir†**	0.0000274	0.0000154	0.0000290	0.0000222	0.0000160
Pt†	0.000618	0.000650	0.000249	0.000158	0.000127
Au	0.000938	0.000800	-	-	-
Hg**	0.0337	0.0300	-	-	-
Tl	0.805	0.500	-	-	-
Pb	16.5	11.7	4.50	8.08	10.8
Bi	0.190	0.0700	-	-	-
Th	10.6	3.68	0.767	2.21	4.90
U	2.64	1.00	0.248	0.621	1.27
Eu/Eu*	0.693	0.830	1.07	0.946	0.848
Heat prod. (nW/kg)	0.623	0.235	0.0640	0.149	0.303
Heat prod. (μW/m^3)	1.81	0.682	0.186	0.432	0.878
Nb/Ta	13.4	13.3	11.7	12.5	12.9
Zr/Hf	35.5	36.0	40.6	37.7	36.6
Th/U	4.00	3.68	3.09	3.56	3.85

K/U	10500	12800	25100	15200	12300
La/Yb	13.7	8.27	6.82	7.63	9.89
Rb/Cs	22.2	36.8	27.2	34.4	25.7
K/Rb	278	272	547	325	301
La/Ta	36.9	33.5	19.4	26.1	0.71

Oxides reported in wt.%. All other abundances reported in ppm.

** denotes elements for which N <6 for middle and/or lower crust

† denotes Upper crustal values from sources other than Gaschnig et al. (2016). Please see text for sources of † abundances.

Table 4. Comparison of Deep Crustal Physical Properties

Model	Vp (km/s)	Vs(km/s)	Vp/Vs	Poiss.	Density (kg/m^3)
Our MC*	6.84	4.04	1.69	0.233	2980
RG MC*	6.74	3.97	1.70	0.235	2940
Low Vp MC†	6.57	3.80	1.73	0.235	2720
CRUST 1.0 MC	6.47	3.70	1.75	0.257	2830
LITHO 1.0 MC	6.51	3.75	1.74	0.252	2840
Our LC**	7.05	4.13	1.71	0.239	3090
RG LC**	7.00	4.01	1.74	0.255	3050
Low Vp LC†	6.80	3.92	1.74	0.235	2920
CRUST 1.0 LC	7.04	4.01	1.76	0.261	3010
LITHO 1.0 LC	7.05	4.00	1.76	0.263	2990
MORB (LC)**	7.40	4.23	1.75	0.258	3260
OIB (LC)**	7.46	4.28	1.74	0.255	3330

† Table 4 Middle Crust Vp 6.5-6.6; Lower Crust 6.7-6.9 (Hacker et al., 2015)

◇ W values from Archean granulite facies terrains (n = 3) excluded as outliers

*MC Conditions - 300 C, 0.4 GPa

**LC Conditions - 500 C, 0.85 GPa

"RG" = Rudnick and Gao (2014)

10 Author Contributions

L.G.S. wrote this text and curated the deep crustal dataset with significant insights and text additions from W.F.M.. All authors have read and approved this manuscript.

Acknowledgments

L.G.S. would like to acknowledge Caerwyn Hartten for her assistance in curating the metamorphic datasets. L.G.S. and W.F.M. would like to acknowledge the NSF for support (grant EAR1650365). Geochemical data were provided by Earthchem.org (`http://www.EarthChem.org/`) and can be found in the supplemental information and here.

References

Arevalo, R., & McDonough, W. F. (2008). Tungsten geochemistry and implications for understanding the earth's interior. *Earth and Planetary Science Letters*, *272*(3-4), 656–665.

Arevalo, R., & McDonough, W. F. (2010, March). Chemical variations and regional diversity observed in MORB. *Chemical Geology*, *271*(1), 70-85. doi: 10.1016/j.chemgeo.2009.12.013

Arevalo, R., McDonough, W. F., & Luong, M. (2009). The k/u ratio of the silicate earth: Insights into mantle composition, structure and thermal evolution. *Earth and Planetary Science Letters*, *278*(3-4), 361–369.

Arndt, N. (1994). Archean komatiites. *Archean crustal evolution*, *10*, 11–44.

Ashwal, L. D., Tucker, R. D., & Zinner, E. K. (1999). Slow cooling of deep crustal granulites and pb-loss in zircon. *Geochimica et Cosmochimica Acta*, *63*(18), 2839–2851.

Banks, D., Green, R., Cliff, R., & Yardley, B. (2000). Chlorine isotopes in fluid inclusions: determination of the origins of salinity in magmatic fluids. *Geochimica et Cosmochimica Acta*, *64*(10), 1785–1789.

Barnes, S.-J. (2016). Chalcophile elements.

Barnhart, K. R., Mahan, K. H., Blackburn, T. J., Bowring, S. A., & Dudas, F. O. (2012). Deep crustal xenoliths from central montana, usa: Implications for the timing and mechanisms of high-velocity lower crust formation. *Geosphere*, *8*(6), 1408–1428.

Bellini, G., Ianni, A., Ludhova, L., Mantovani, F., & McDonough, W. F. (2013). Geo-neutrinos. *Progress in Particle and Nuclear Physics*, *73*, 1–34.

Bohlen, S., & Mezger, K. (1989). Origin of granulite terranes and the formation of the lowermost continental crust. *Science*, *244*(4902), 326–329.

Brocher, T. M. (2005, December). Empirical Relations between Elastic Wavespeeds and Density in the Earth's Crust. *Bulletin of the Seismological Society of America*, *95*(6), 2081-2092. doi: 10.1785/0120050077

Brown, M., & Johnson, T. (2019). Time's arrow, time's cycle: Granulite metamorphism and geodynamics. *Mineralogical Magazine*, *83*(3), 323–338.

Bürgmann, R., & Dresen, G. (2008). Rheology of the lower crust and upper mantle: Evidence from rock mechanics, geodesy, and field observations. *Annu. Rev. Earth Planet. Sci.*, *36*, 531–567.

Chappell, B. W., Bryant, C. J., & Wyborn, D. (2012). Peraluminous i-type granites. *Lithos*, *153*, 142–153.

Charlier, B., Namur, O., Toplis, M. J., Schiano, P., Cluzel, N., Higgins, M. D., & Auwera, J. V. (2011). Large-scale silicate liquid immiscibility during differentiation of tholeiitic basalt to granite and the origin of the daly gap. *Geology*, *39*(10), 907–910.

Chen, K., Rudnick, R. L., Wang, Z., Tang, M., Gaschnig, R. M., Zou, Z., ... Liu, Y. (2020). How mafic was the archean upper continental crust? insights from cu and ag in ancient glacial diamictites. *Geochimica et Cosmochimica Acta*, *278*, 16–29.

Chen, K., Walker, R. J., Rudnick, R. L., Gao, S., Gaschnig, R. M., Puchtel, I. S., ... Hu, Z.-C. (2016). Platinum-group element abundances and re–os isotopic systematics of the upper continental crust through time: Evidence from glacial diamictites. *Geochimica et Cosmochimica Acta*, *191*, 1–16.

Christensen, N. I., & Mooney, W. D. (1995). Seismic velocity structure and composition of the continental crust: A global view. *Journal of Geophysical Research: Solid Earth*, *100*(B6), 9761-9788. doi: 10.1029/95JB00259

Daly, R. (1914). Igneous rocks and their origin. *Preliminary Note on Alkaline Rhyolites from Tokati, Hokkaido*, *319*, 20.

De Argollo, R., & Schilling, J.-G. (1978). Ge/si and ga/al fractionation in hawaiian volcanic rocks. *Geochimica et Cosmochimica Acta*, *42*(6), 623–630.

De La Roche, d. H., Leterrier, J. t., Grandclaude, P., & Marchal, M. (1980). A classification of volcanic and plutonic rocks using r1r2-diagram and major-element analysesits relationships with current nomenclature. *Chemical geology*, *29*(1-4), 183–210.

Dufek, J., & Bachmann, O. (2010). Quantum magmatism: Magmatic compositional gaps generated by melt-crystal dynamics. *Geology*, *38*(8), 687–690.

Farcy, B., Arevalo, R., & McDonough, W. (2020). K/u of the morb source and silicate earth. *Journal of Geophysical Research: Solid Earth*, *125*(12), e2020JB020245.

Field, D., & Clough, P. W. (1976). K/rb ratios and metasomatism in metabasites from a precambrian amphibolite–granulite transition zone. *Journal of the Geological Society*, *132*(3), 277–288.

Field, D., & Elliott, R. (1974). The chemistry of gabbro/amphibolite transitions in south norway. *Contributions to Mineralogy and Petrology*, *47*(1), 63–76.

Fowler, M. (1986). Large-ion lithophile element characteristics of an amphibolite facies to granulite facies transition at gruinard bay, north-west scotland. *Journal of Metamorphic Geology*, *4*(3), 345–359.

Gale, A., Laubier, M., Escrig, S., & Langmuir, C. H. (2013). Constraints on melting processes and plume-ridge interaction from comprehensive study of the famous and north famous segments, mid-atlantic ridge. *Earth and Planetary Science Letters*, *365*, 209–220.

Gao, S., Zhang, B.-R., Jin, Z.-M., Kern, H., Luo, T.-C., & Zhao, Z.-D. (1998). How mafic is the lower continental crust? *Earth and Planetary Science Letters*, *161*(1-4), 101–117.

Gard, M., Hasterok, D., Hand, M., & Cox, G. (2019). Variations in continental heat production from 4 ga to the present: Evidence from geochemical data. *Lithos*, *342*, 391–406.

Gaschnig, R. M., Rudnick, R. L., McDonough, W. F., Kaufman, A. J., Valley, J. W., Hu, Z., ... Beck, M. L. (2016). Compositional evolution of the upper continental crust through time, as constrained by ancient glacial diamictites. *Geochimica et Cosmochimica Acta*, *186*, 316–343.

Gerya, T. V., Perchuk, L. L., & Burg, J.-P. (2008). Transient hot channels: perpetrating and regurgitating ultrahigh-pressure, high-temperature crust–mantle associations in collision belts. *Lithos*, *103*(1-2), 236–256.

Gerya, T. V., Perchuk, L. L., Maresch, W. V., Willner, A. P., Reenen, D. D. V., & Smit, C. A. (2002). Thermal regime and gravitational instability of multilayered continental crust: implications for the buoyant exhumation of high-grade metamorphic rocks. *European Journal of Mineralogy*, *14*(4), 687–699.

Godfrey, N. J., Christensen, N. I., & Okaya, D. A. (2000). Anisotropy of schists: Contribution of crustal anisotropy to active source seismic experiments and shear wave splitting observations. *Journal of Geophysical Research: Solid Earth*, *105*(B12), 27991–28007.

Hacker, B. R., Kelemen, P. B., & Behn, M. D. (2015). Continental Lower Crust. *Annual Review of Earth and Planetary Sciences*, *43*(1), 167-205. doi: 10.1146/annurev-earth-050212-124117

Halliday, A. N., Dickin, A. P., Hunter, R. N., Davies, G. R., Dempster, T. J., Hamilton, P. J., & Upton, B. G. J. (1993). Formation and composition of the lower continental crust: Evidence from Scottish xenolith suites. *Journal of Geophysical Research: Solid Earth*, *98*(B1), 581-607. doi: 10.1029/92JB02276

Hartigan, J. A., & Hartigan, P. M. (1985). The dip test of unimodality. *The annals of Statistics*, *13*(1), 70–84.

Hasterok, D., Gard, M., Bishop, C., & Kelsey, D. (2019). Chemical identification of metamorphic protoliths using machine learning methods. *Computers & Geosciences*, *132*, 56–68.

Hasterok, D., Gard, M., Cox, G., & Hand, M. (2019). A 4 ga record of granitic heat

production: Implications for geodynamic evolution and crustal composition of the early earth. *Precambrian Research*, *331*, 105375.

Holbrook, W. S., Mooney, W. D., & Christensen, N. I. (1992). The seismic velocity structure of the deep continental crust. *Continental lower crust*, *23*, 1–43.

Huang, Y., Chubakov, V., Mantovani, F., Rudnick, R. L., & McDonough, W. F. (2013). A reference Earth model for the heat-producing elements and associated geoneutrino flux. *Geochemistry, Geophysics, Geosystems*, *14*(6), 2003-2029. doi: 10.1002/ggge.20129

Jackson, M., Blundy, J., & Sparks, R. (2018). Chemical differentiation, cold storage and remobilization of magma in the earths crust. *Nature*, *564*(7736), 405–409.

Jaupart, C., & Mareschal, J. (2003). *Constraints on heat production from heat flow data, treatise on geochemistry, vol. 3, the crust, edited by r. rudnick.* Elsevier Sci., New York.

Jenner, F. E. (2017). Cumulate causes for the low contents of sulfide-loving elements in the continental crust. *Nature Geoscience*, *10*(7), 524–529.

Kelemen, P. B., & Behn, M. D. (2016). Formation of lower continental crust by relamination of buoyant arc lavas and plutons. *Nature Geoscience*, *9*(3), 197–205.

Kusebauch, C., John, T., Barnes, J. D., Klügel, A., & Austrheim, H. O. (2015). Halogen element and stable chlorine isotope fractionation caused by fluid–rock interaction (bamble sector, se norway). *Journal of Petrology*, *56*(2), 299–324.

Kusznir, N., & Park, R. (1987). The extensional strength of the continental lithosphere: its dependence on geothermal gradient, and crustal composition and thickness. *Geological Society, London, Special Publications*, *28*(1), 35–52.

Laske, G., Ma, Z., Masters, G., & Pasyanos, M. (2016). *Crust 1.0: a new global crustal model at 1x1 degrees.*

Leech, M. L. (2001, February). Arrested orogenic development: Eclogitization, delamination, and tectonic collapse. *Earth and Planetary Science Letters*, *185*(1), 149-159. doi: 10.1016/S0012-821X(00)00374-5

Lombardo, B., & Rolfo, F. (2000, February). Two contrasting eclogite types in the Himalayas: Implications for the Himalayan orogeny. *Journal of Geodynamics*, *30*(1), 37-60. doi: 10.1016/S0264-3707(99)00026-5

MacDonald, G. A., & Katsura, T. (1964). Chemical composition of hawaiian lavas. *Journal of petrology*, *5*(1), 82–133.

Markl, G., Musashi, M., & Bucher, K. (1997). Chlorine stable isotope composition of granulites from lofoten, norway: Implications for the cl isotopic composition and for the source of cl enrichment in the lower crust. *Earth and Planetary Science Letters*, *150*(1-2), 95–102.

Martin, H. (1986). Effect of steeper archean geothermal gradient on geochemistry of subduction-zone magmas. *Geology*, *14*(9), 753–756.

McDonough, W. F. (1990). Constraints on the composition of the continental lithospheric mantle. *Earth and Planetary Science Letters*, *101*(1), 1–18.

McDonough, W. F. (1991). Partial melting of subducted oceanic crust and isolation of its residual eclogitic lithology. *Philosophical Transactions of the Royal Society of London. Series A: Physical and Engineering Sciences*, *335*(1638), 407–418.

McDonough, W. F., & Sun, S.-s. (1995, March). The composition of the Earth. *Chemical Geology*, *120*(3), 223-253. doi: 10.1016/0009-2541(94)00140-4

Mooney, W. D., Laske, G., & Masters, T. G. (1998, January). CRUST 5.1: A global crustal model at 5◦ x 5◦. *Journal of Geophysical Research: Solid Earth*, *103*(B1), 727-747. doi: 10.1029/97JB02122

Ohta, T., & Arai, H. (2007). Statistical empirical index of chemical weathering in igneous rocks: A new tool for evaluating the degree of weathering. *Chemical Geology*, *240*(3-4), 280–297.

Palme, H., & O'Neill, H. S. C. (2014). Cosmochemical estimates of mantle com-

position. In H. D. Holland & K. K. Turekian (Eds.), *Treatise on geochemistry (second edition)* (Vol. 3, pp. 1–39). Oxford: Elsevier. doi: 10.1016/B978-0-08-095975-7.00201-1

Pasyanos, M. E., Masters, T. G., Laske, G., & Ma, Z. (2014, March). LITHO1.0: An updated crust and lithospheric model of the Earth. *Journal of Geophysical Research: Solid Earth*, *119*(3), 2153-2173. doi: 10.1002/2013JB010626

Polat, A., Hofmann, A., & Rosing, M. T. (2002). Boninite-like volcanic rocks in the 3.7–3.8 ga isua greenstone belt, west greenland: geochemical evidence for intra-oceanic subduction zone processes in the early earth. *Chemical geology*, *184*(3-4), 231–254.

Price, J. R., & Velbel, M. A. (2003). Chemical weathering indices applied to weathering profiles developed on heterogeneous felsic metamorphic parent rocks. *Chemical geology*, *202*(3-4), 397–416.

Reubi, O., & Blundy, J. (2009, October). A dearth of intermediate melts at subduction zone volcanoes and the petrogenesis of arc andesites. *Nature*, *461*(7268), 1269-1273. doi: 10.1038/nature08510

Rockow, K. M., Haskin, L. A., Jollif, . B., & Fountain, D. M. (1997). Constraints on element mobility associated with the conversion of granulite to eclogite along fractures in an anorthositic complex on holsnøy, norway. *Journal of Metamorphic Geology*, *15*(3), 401–418.

Rogers, N., & Hawkesworth, C. (1982). Proterozoic age and cumulate origin for granulite xenoliths, lesotho. *Nature*, *299*(5882), 409–413.

Rudnick, R. L. (1995). Making continental crust. *Nature*, *378*(6557), 571–578.

Rudnick, R. L., Barth, M., Horn, I., & McDonough, W. F. (2000). Rutile-bearing refractory eclogites: missing link between continents and depleted mantle. *Science*, *287*(5451), 278–281.

Rudnick, R. L., & Fountain, D. M. (1995). Nature and composition of the continental crust: A lower crustal perspective. *Reviews of Geophysics*, *33*(3), 267-309. doi: 10.1029/95RG01302

Rudnick, R. L., & Gao, S. (2014). Composition of the Continental Crust. In *Treatise on Geochemistry* (p. 1-51). Elsevier. doi: 10.1016/B978-0-08-095975-7.00301-6

Rudnick, R. L., McLennan, S. M., & Taylor, S. R. (1985). Large ion lithophile elements in rocks from high-pressure granulite facies terrains. *Geochimica et Cosmochimica Acta*, *49*(7), 1645–1655.

Rudnick, R. L., & Presper, T. (1990). Geochemistry of intermediate/-to high-pressure granulites. In *Granulites and crustal evolution* (pp. 523–550). Springer.

Rudnick, R. L., & Taylor, S. R. (1987a). The composition and petrogenesis of the lower crust: a xenolith study. *Journal of Geophysical Research: Solid Earth*, *92*(B13), 13981–14005.

Rudnick, R. L., & Taylor, S. R. (1987b, December). The composition and petrogenesis of the lower crust: A xenolith study. *Journal of Geophysical Research: Solid Earth*, *92*(B13), 13981-14005. doi: 10.1029/JB092iB13p13981

Russell, J. K., Porritt, L. A., Lavallée, Y., & Dingwell, D. B. (2012). Kimberlite ascent by assimilation-fuelled buoyancy. *Nature*, *481*(7381), 352–356.

Semprich, J., & Simon, N. S. C. (2014, March). Inhibited eclogitization and consequences for geophysical rock properties and delamination models: Constraints from cratonic lower crustal xenoliths. *Gondwana Research*, *25*(2), 668-684. doi: 10.1016/j.gr.2012.08.018

Shinevar, W. J., Behn, M. D., Hirth, G., & Jagoutz, O. (2018, July). Inferring crustal viscosity from seismic velocity: Application to the lower crust of Southern California. *Earth and Planetary Science Letters*, *494*, 83-91. doi: 10.1016/j.epsl.2018.04.055

Sighinolfi, G. P. (1971). Investigations into deep crustal levels: fractionating ef-

fects and geochemical trends related to high-grade metamorphism. *Geochimica et Cosmochimica Acta*, *35*(10), 1005–1021.

Stosch, H.-G., Lugmair, G., & Seck, H. (1986). Geochemistry of granulite-facies lower crustal xenoliths: implications for the geological history of the lower continental crust below the eifel, west germany. *Geological Society, London, Special Publications*, *24*(1), 309–317.

Sun, S., & McDonough, W. F. (1989, January). Chemical and isotopic systematics of oceanic basalts: Implications for mantle composition and processes. *Geological Society, London, Special Publications*, *42*(1), 313-345. doi: 10.1144/GSL.SP.1989.042.01.19

Svensen, H., Jamtveit, B., Banks, D. A., & Austrheim, H. (2001). Halogen contents of eclogite facies fluid inclusions and minerals: Caledonides, western norway. *Journal of Metamorphic Geology*, *19*(2), 165–178.

Tang, M., McDonough, W. F., & Ash, R. D. (2017). Europium and strontium anomalies in the morb source mantle. *Geochimica et Cosmochimica Acta*, *197*, 132–141.

Taylor, S. R., & McLennan, S. M. (1985). *The continental crust: its composition and evolution*. Blackwell Scientific Pub., Palo Alto, CA.

Tsujimori, T., Sisson, V. B., Liou, J. G., Harlow, G. E., & Sorensen, S. S. (2006). Very-low-temperature record of the subduction process: A review of worldwide lawsonite eclogites. *Lithos*, *92*(3-4), 609–624.

Wedepohl, K. H. (1995). The composition of the continental crust. *Geochimica et cosmochimica Acta*, *59*(7), 1217–1232.

Wipperfurth, S. A., Guo, M., Šrámek, O., & McDonough, W. F. (2018, September). Earth's chondritic Th/U: Negligible fractionation during accretion, core formation, and crust–mantle differentiation. *Earth and Planetary Science Letters*, *498*, 196-202. doi: 10.1016/j.epsl.2018.06.029

Wipperfurth, S. A., Šrámek, O., & McDonough, W. F. (2020). Reference Models for Lithospheric Geoneutrino Signal. *arXiv:1907.12184 [physics]*.

Yamasaki, T. (2018). The role of bimodal magmatism in seafloor massive sulfide (sms) ore-forming systems at the middle okinawa trough, japan. *Ocean Science Journal*, *53*(2), 413–436.

Zen, E.-A. (1988). Phase relations of peraluminous granitic rocks and their petrogenetic implications. *Annual Review of Earth and Planetary Sciences*, *16*(1), 21–51.